

Macro-scale Computational Analysis of the *Hydro Filtterra* Storm Water Drainage System in an Industrial Urban Environment

For Group Project:

Investigating Stormwater Filters and Bioretention Systems

A Study on the *Hydro Filtterra*[™] System Manufactured by *Hydro International (UK)*



Individual Report – I2

2012

Jon Tarrant

Candidate Number: 030958

Student ID: 570013341

Supervisor: Dr Gavin Tabor

I: Abstract

This report describes the individual responsibilities and contributions of Jon Tarrant within the Group Project 'Investigating Stormwater Filters and Bioretention Systems'.

With an increasing demand for industry to limit its impact on the environment, and for infrastructure to cope with those demands, it is vital that sustainable methods of water purification are developed. To this end, *Hydro International* has developed the *Hydro Filtterra* bioretention system, an organic application designed to treat storm water and surface run-off in urban development locations.

This project analysed the *Hydro Filtterra* unit at the macro level using computational methods, examining its fluid behaviour with a view to optimising the system. Analysis included multiphase / free surface flow through porous media and demonstrates a thorough understanding of the Computational Fluid Dynamics software *OpenFOAM*, its mathematical principles and operation. The results of these investigations have been delivered to the group project and to *Hydro International* with whom this project has been completed.

Keywords: CFD, Free Surface Flow, Urban Stormwater Drainage

II: Table of Contents

I: Abstract.....	I
II: Table of Contents.....	II
III: List of Figures	III
IV: List of Tables	III
1. Introduction & Overview	1
1.1 The Need for Storm Water Management.....	1
1.2 The <i>Hydro Filterra</i> Bioretention System.....	1
1.3 Group Project Overview	2
1.4 Individual Project Overview	2
2. Research & Previous Work	3
2.1 1D & 2D Urban Drainage Simulation	3
2.2 3D Modelling of Urban Drainage & Water Management Systems.....	5
3. Methodology & Mathematical Foundation	8
3.1 Project Plan.....	9
3.2 Computational Fluid Dynamics & <i>OpenFOAM</i>	9
3.3 Mathematical Approach to Free Surface Flow	10
4. Two-Dimensional Modelling	12
4.1 Initial 2D Inlet Case	13
4.1.1 2D Inlet Geometry & Mesh Generation	13
4.1.2 Boundary Conditions.....	14
4.1.3 Applying Different Turbulence Models.....	17
4.1.4 Mesh Refinement.....	18
4.2 The Addition of a Porous Zone.....	19
4.3 The Influence of the Energy Dissipation Layer.....	20
4.4 Summary & Discussion of 2D Modelling	23
5. Three-Dimensional Modelling.....	24
5.1 3D Inlet Case Simulation.....	24
5.2 3D Cross-Flow Case Simulation.....	25
6. Collaborative Work & Final 3D Simulation	28
7. Conclusions & Discussion	31
8. Project Evaluation & Further Work	31
References.....	33

III: List of Figures

Fig. 1 – The <i>Hydro Filterra</i> Bioretention System [1, 5]	2
Fig. 2 a) Contours of U/U_{mean} for circular pipe with $h/D = 0.7$ and b) percentage error between numerical and empirical data	5
Fig. 3 – Graph of Relative Vertical Position in Water against Velocity – the ‘Dip Phenomenon’ ..	6
Fig. 4 – Alternative Mechanical Storm Water Filtration Units	6
Fig. 5 – Experimental Set-up for the Gulley Drainage Case	7
Fig. 6 – CFD Simulation of Gulley Pot Including Streamlines [10]	8
Fig. 7 – Cross-section of the <i>Hydro Filterra</i> bioretention unit	13
Fig. 8 – Initial 2D Inlet Geometry.....	13
Fig. 9 – First Mesh for Initial 2D Inlet Case.....	14
Fig. 10 – <i>Alpha1</i> Field for Initial 2D Inlet	16
Fig. 11 – Mesh Refinement Process.....	18
Fig. 12 – U_y Velocity Field for Mesh Refinement 5.....	18
Fig. 13 – <i>Alpha1</i> Field for mesh Refinement 1 (left) and 5 (right)	19
Fig. 14 – Original Inlet with Porous Zones.....	20
Fig. 15 – Slab Options 1 (left) and 2 (right).....	20
Fig. 16 – <i>Alpha1</i> & U Magnitude Plot for Initial 2D Model.....	21
Fig. 17 – Development of <i>Alpha1</i> Field in Porous Zones for Original Design.	21
Fig. 18 – <i>Alpha1</i> Field Progression for Slab Variation 1.....	22
Fig. 19 – <i>Alpha1</i> Field Propagation in Slab Variation 2	22
Fig. 20 – <i>Alpha1</i> Field For 3-Dimensional Case	24
Fig. 21 – Mesh for 3D Cross-Flow Case Simulation	25
Fig. 22 – Boundary Condition for <i>Alpha1</i> (left) and Velocity U_z (right).....	26
Fig. 23 – U_x Field at $t=0.05s$	26
Fig. 24 – <i>Alpha1</i> Field Progression in 3D with Street Drainage	27
Fig. 25 – View of <i>Alpha1</i> Field from beneath Simulated Domain	27
Fig. 26 – <i>Alpha1</i> Field Adjacent to Drain Inlet Clockwise (from top left) $t=2, 4, 8$ and $6s$	28
Fig. 27 – Full 3D Simulation Mesh with Inlets, Outlet Pipe and Roots	30
Fig. 28 – Slice from 3D Simulation Displaying <i>Alpha1</i> Field	30

IV: List of Tables

Table 1 – Mesh Refinement Table.....	18
Table 2 – Energy Dissipation Layer Design Comparison Table	23
Table 3 – Boundary Condition Changes for 3D Cross-Flow Case	25
Table 4 – <i>SnappyHexMesh</i> Process	29

1. Introduction & Overview

This report describes the individual responsibilities and contributions of Jon Tarrant within the Group Project 'Investigating Stormwater Filters and Bioretention Systems'. A small proportion of the material covered has been discussed in other works by this author for the overall project [1-3], and are included for clarity. Collaborative works with other group members are cited where necessary.

The individual element of the project examines the fluid behaviour at the macro-level of storm water flow and surface run-off into and around the Hydro Filterra bioretention filter system. Such products can be utilised in a variety of urban and industrial locations in order to lessen the impact of this type of infrastructure on the wider hydrological cycle.

1.1 The Need for Storm Water Management

Increased awareness of the environmental impact of human activity is driving a new era of responsibility and sustainability. It is desirable therefore that, as far as reasonably practicable, the effect of urban development on the local ecosystem should be minimised.

To this end, the Water Framework Directive (WFD), adopted by the EU in October 2000, requires that surface-water management across Europe should meet specified cleanliness criteria. This directive aims to bring a greater focus to environmental considerations and sustainability. In 2003, this directive was adopted to UK policy.

The purification of waste water involves the removal of both macro and micro scale pollutants. In urban areas in particular, storm water can become contaminated with chemical pollutants and particulate matter. It is important to filter out such pollutants before the water can be re-introduced to the main supply. Typically, this process is completed at water treatment plants towards the end of the sewerage system. With the advent of bioretention systems however, the majority of this process can be completed at the point where the water enters the system, thus easing the demand on water treatment and purification plants. This can be achieved using mechanical and / or biological systems such as the *Hydro Filterra* system analysed in this project.

With the introduction to UK policy of the Sustainable Urban Drainage Systems (SUDS) policy in 2012, the usage of such filtration systems will greatly increase. The focus of this legislation is the use of natural systems, to treat and clean storm water run-off. Such designs do not require energy input from the national grid, reduce the pressure on the existing infrastructure, minimise incidence of flooding and can be aesthetically pleasing.

1.2 The *Hydro Filterra* Bioretention System

Hydro International, founded in 1980 specialises in products for the cost effective control of stormwater and treatment of wastewater [4], such as the *Hydro Filterra* bioretention system, which directly addresses the issues detailed above. As with other bioretention systems, *Hydro Filterra* utilises the behaviour inherent in porous biological media to filter and clean chemical pollutants from surface run-off whilst regulating the volumetric flow.

Hydro Filtterra has significant advantages over its competitors since it occupies a smaller footprint and utilises a specially engineered soil to optimise filtration. Despite its small size, it still satisfies the WFD and SUDS legislation. A representative diagram of a *Hydro Filtterra* system is given in Fig. 1, below.

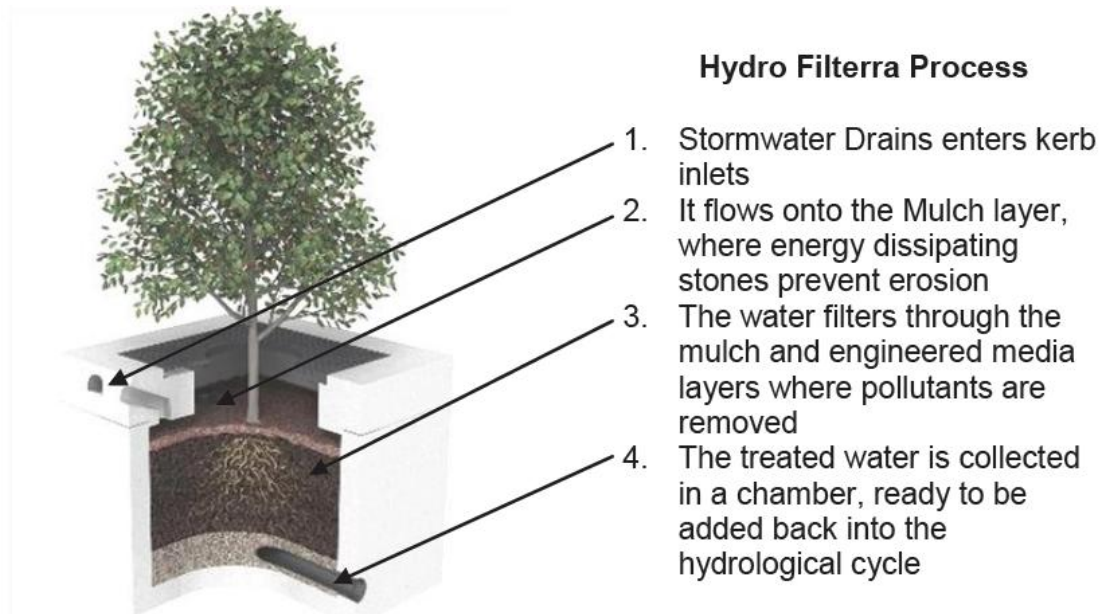


Fig. 1 – The *Hydro Filtterra* Bioretention System [1, 5]

1.3 Group Project Overview

The overall objective of this project was to analyse, experimentally and computationally, the hydrodynamic behaviour of storm-water flow and surface run-off into and around the *Hydro Filtterra* bioretention system. The specific aim was to determine, and subsequently optimise, the operational parameters of this system. The results of this project will be forwarded to *Hydro International*, with whom this project will be closely associated.

Successful delivery of this project will be achieved through analysing a single case study example of the *Hydro Filtterra* system currently installed in Barry, South Wales. Both experimental and numerical approaches have been adopted by the group to ensure rigorous analysis of the system and the project group has been divided into two teams to reflect this division. This author is involved in the computational fluid dynamics (CFD) team. Thorough discussion concerning division of labour within the project is defined in the Group Reports G1 and G2 [1, 3].

1.4 Individual Project Overview

This project concerns the macro-level fluid interface at the inlet of the *Hydro Filtterra* bioretention system. The fluid flow will be comprehensively modelled and analysed using different flow conditions, transient effects and time-dependent flow behaviours. The models should represent accurately the currently installed *Hydro Filtterra* systems in Barry in terms of geometry, model inputs and other physical constraints. This will ensure that any computational analysis can be verified against the available empirical data. This project will be undertaken using *OpenFOAM*, an open-source CFD code.

The main individual project objectives and deliverables as outlined in the I1 report [2] were:

Objectives

- Successfully generate 2D and 3D simulations of the *Hydro Filtterra* unit including the surface run-off adjacent to the system and inlet flow including porous media, with particular focus on optimising the installation
- Combine these elements with the work of Pavey and Ronald [6, 7] to generate a full-scale 3D model of the filtration unit
- Areas of further study may include multi-phase flow for contaminants such as diesel

Deliverables

- 2D and 3D *OpenFOAM* models of surface run-off into the unit from the Barry case study featuring a number of different transient flow conditions and free surface effects
- A full macro model of the entire system including the internal media, featuring a number of different flow conditions

2. Research & Previous Work

Computational Fluid Dynamics (CFD) is a powerful tool commonly associated with Computer Aided Engineering (CAE) tasks in a wide range of fluid behavioural problems not least in the field of urban drainage. The following sections of this report summarise the research work that was conducted as part of the I1 report for this project. Different CFD codes and software that have been applied to resolve fluid flow issues which are common to this industry have been investigated. Extensive research has been completed into the drainage behaviour of surface run-off [8, 9] and the effects of heavy rainfall events and flooding [10]. Many studies have also been completed to validate the numerical simulations against their experimental counterparts [11-13].

2.1 1D & 2D Urban Drainage Simulation

Storm Water Management Model (SWMM) software is commonly used to generate 1D and 2D models of urban drainage situations. Two specific cases [8, 9] have been examined which present simulations demonstrating the capability of this software in modelling fluid flow in surface / subsurface interaction, a key area of investigation for the present project.

In the first case, an urban environment representative of a city such as Paris or Montpellier has been analysed and resolved using both 1D and 2D approaches. The aim of the investigation was to determine the numerical differences between the two approaches and to establish the capacity of 1D simulation to compute surface flows.

Numerical stability was assured through the implementation of different combinations of transient inputs to the model, namely 'gradual' and 'brutal' flow injections at the street and sewer networks. 'Gradual' inputs gave a simple transitional gradient from $0.01\text{m}^3\text{s}^{-1}$ to $15\text{m}^3\text{s}^{-1}$. 'Brutal' inputs were described by a step input between these two values.

It was found that a simple 1D representation can show good agreement to a more complex 2D model with regard to surface flow and interaction between the surface and sewer networks. Indeed, it was shown that the comparison in 1D and 2D yielded a consistent difference ratio of 0.7. The reason for this difference is cited as the energy dissipation due to confluence at the crossroad sections, which is clearly unaccounted for in the 1D model.

These data were also compared with experimental results from another study [14] and showed good correlation with regard to discharge rates and manhole operation and efficiency. It was proposed that further tests should be conducted to improve agreement with the experimental data. A function that accounts for energy dissipation at crossroads should also be investigated.

Another study [9] was conducted in order to determine the effectiveness of 1D/1D and 1D/2D modelling for surface / sub-surface interaction. 1D/1D modelling considers the two domains (surface and sewer) as one-dimensional regions. The 1D/2D model represents the surface model as a two-dimensional region. Linking the two regions is vital to development of urban water management models as there are many different physical interactions between these two regions which dictate heavy rainfall and flooding events. Comparison with experimental data for a specific case study was used as validation of the simulation.

Both models were carefully constructed so that the physical inputs were matched for the same geometry and section of the sewer network. The computational expertise of the modeller was recognised as one of the key features that increase the difficulty of such comparative studies. Furthermore, careful attention should be paid to the physical constraints placed on the system.

Typically, the required parameters for the experimentation between the two cases would be water depth and velocity. Since the 1D/2D model has two components for the velocity instead of the 1D/1D singular velocity, the depth and arrival time of the flood waves are observed. This was assumed to infer the flood behaviour [9].

The two versions of the model were comprehensively tested and examined and yielded notable results. It was shown that the 1D/1D model can provide good agreement with the 1D/2D model, but this was only after careful calibration of each model, matching the inlet and outlet flow rates. The advantage of the 1D/1D system is that it utilises unconditionally stable finite difference methods and is computationally inexpensive, particularly when compared to the 1D/2D model.

In general, it was observed that SWMM can yield good agreement with experimental data, but highlighted the necessity for computational accuracy of the modeller with regard to inlet / outlet conditions and definition of phenomena such as ponds, sewer network connections and virtual constraints that adjust the physical behaviour of the system.

The previously described SWMM models have highlighted vital concerns with regard to computational accuracy. Since the proposed work concerns the fluid flow at the point of surface / subsurface interaction, some of these conditions can however be neglected, such as network connections and biaxial flow convergence as these take place within the sewerage network and only affect the surface flow in surcharge conditions [10].

2.2 3D Modelling of Urban Drainage & Water Management Systems

SWMM is a very effective computational code which can be used to analyse urban drainage cases on a very large scale, but due to its large virtual size (that of a city or similar urban environment), it is often limited to two dimensions. The present work however, is concerned with the fluid flow at the point of surface / subsurface interaction and as a result, investigations using more appropriate CFD codes have been examined.

The following section cites three cases [10, 15-16], within which a three-dimensional CFD model has been required to analyse a product or design problem in the field of urban drainage and water management. The first of these cases compares two 3D turbulent flow models with a view to optimising sewerage instrumentation [16]. It is initially proposed that a combination of different velocity components can be combined to determine the mean velocity formula based on the geometrical (rectangular, circular or elliptical) properties of the channel. Through initial testing of this proposed method, whilst the mean velocity was accurate towards the centre of the pipe, there was in excess of a 15% inaccuracy at the wall, demonstrated in Fig. 2.

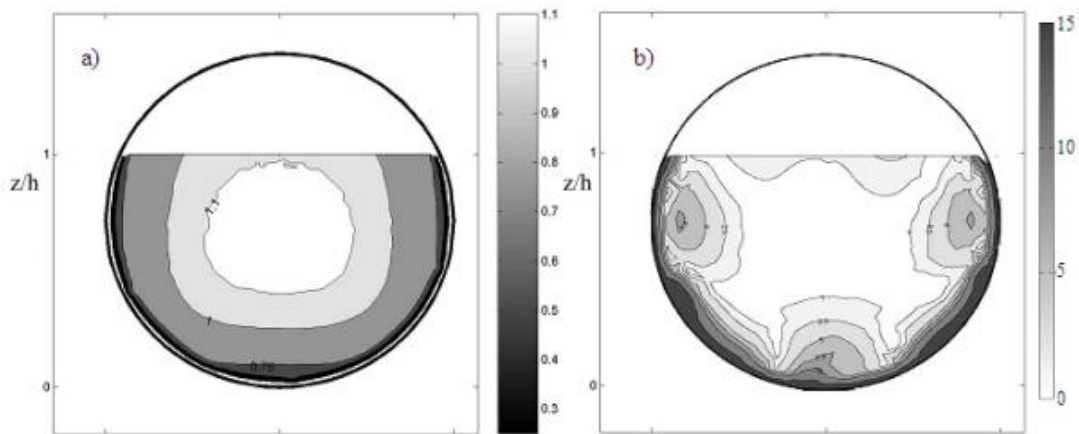


Fig. 2 a) Contours of U/U_{mean} for circular pipe with $h/D = 0.7$ and b) percentage error between numerical and empirical data

In order to simplify the proposed channel evaluation method, a rectangular sewer channel is considered and a turbulent $k-\epsilon$ model is adopted to determine the velocity profile in each plane of the channel with a free surface condition. Implementation of the $k-\epsilon$ model on this channel yielded an isotropic velocity field, but this does not accurately represent the flow in the channel as it does not allow for secondary currents which create anisotropic turbulence. These secondary currents are the result of the free surface interaction and create the dip-phenomenon [16], whereby the maximum velocity is not at the free surface, but just below it. This is demonstrated in Fig. 3.

The red line in Fig. 3 represents the measured velocity of the partially filled channel height, and the dotted blue line represents the flow profile predicted by the $k-\epsilon$ turbulence method. It is clear therefore that an anisotropic turbulence model should be adopted in order to fully describe the flow in the channel, as the mean flow is greatly affected by these secondary currents. In the figure, z/b represents the ratio of the vertical position in the water (z) with regard to the total water depth (b). The axial velocity is expressed as V , represented in the x-axis.

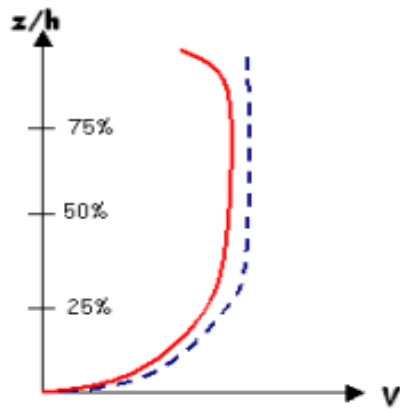


Fig. 3 – Graph of Relative Vertical Position in Water against Velocity – the ‘Dip Phenomenon’

The second case examines the behaviour of four types of storm water filtration units. Increasingly throughout urban drainage, more sophisticated filtration systems are required to remove particulate matter from surcharge flows. The drainage systems observed are namely simple catch basin (SCB), a gravity sedimentation device (GSD), a simple vortex separator (SVS) and an advanced vortex separator (AVS). Fig. 4 presents a graphical illustration of each of these systems [15].

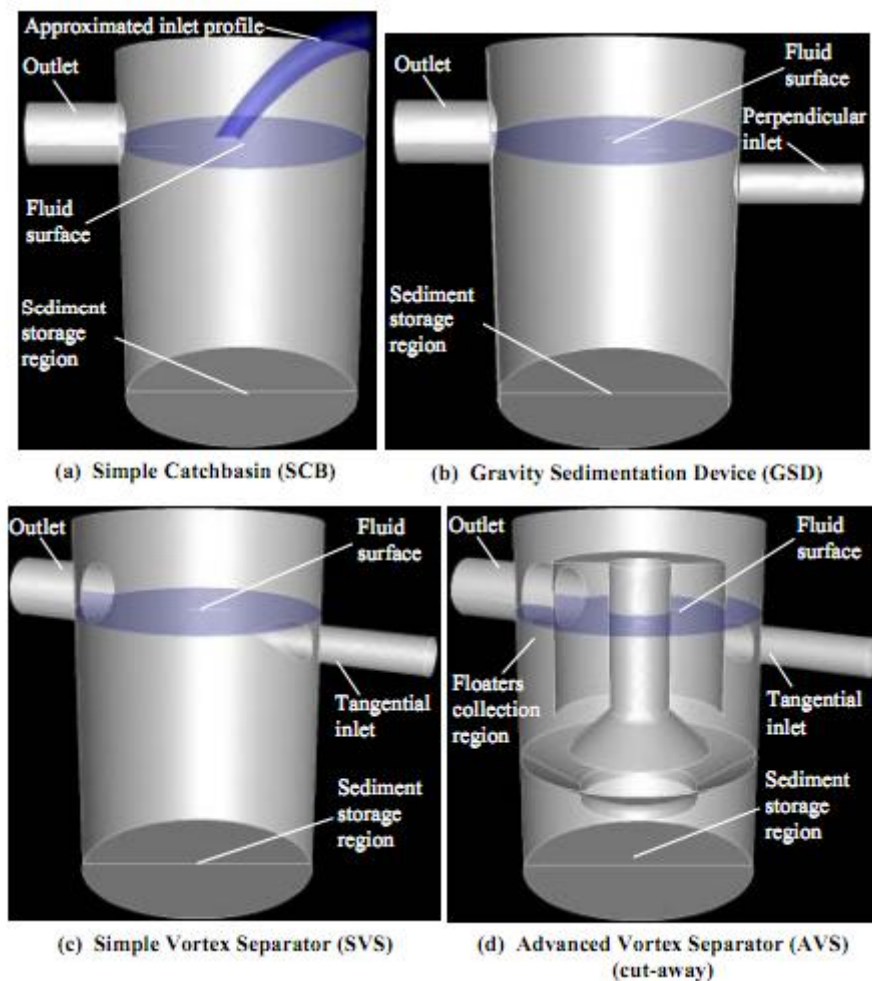


Fig. 4 – Alternative Mechanical Storm Water Filtration Units

Both the general velocities and flow pathlines were considered in the above analysis for a number of different initial volumetric flow rates. The following conclusions were drawn from the analysis.

There is an increasing need for “flow through” stormwater treatment devices to remove sediments and other pollutants from surface run off. The catch basin method of stormwater discharge has been shown to result in a phenomenon referred to as ‘wash-out’, whereby previously removed pollutants re-infiltrate into the outlet flow and pollute the outlet pipe. The analysis of the flow through devices can be summarised by the following key points:

- The geometry and configuration of stormwater treatment chambers has a major impact on the modelled particle removal rates and their respective retention efficiencies.
- The particle retention rates for the Simple Catch Basin case are the worst of those considered. Vortex retention rates are considered to be the most efficient both in terms of particle removal and retention efficiencies.
- Isolation of the sediment storage region from the main treatment region is predicted to have a significant impact on the resulting ability of a chamber to retain collected particles at high flow-rates.

The final case study in this section addresses directly the CFD problem that has been proposed in the general content of this report [10]. Specifically, it addresses the behaviour of sewer interaction with surface flow in a fully three-dimensional surcharge flood scenario. A computational model was established in order to match a full-scale experimental rig set up at the University of Sheffield. The specific area of focus was the flooding of sewer inlets.

Pressure transducers were used in an experimental rig of roughly 2m x 5m and the depth of the water at 6 specific points around the gulley inlet were monitored for their behaviour through surcharging conditions. The experimental set-up is displayed in Fig. 5, below.



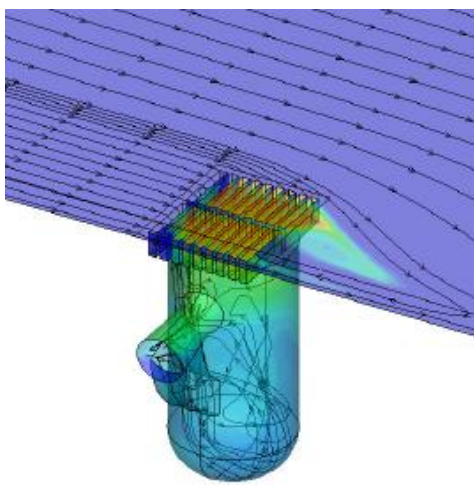
Fig. 5 – Experimental Set-up for the Gully Drainage Case

The rig in Fig. 5 is capable of replicating different gradients in the transverse and axial directions in order to replicate different drainage scenarios. This rig was then simulated in a CFD model as described in the following section.

All experimental data were recorded in real time and the results analysed to establish the conventional coefficient of discharge using a standard weir equation.

OpenFOAM, an open source CFD was utilised to model the urban drainage case as described above. (*OpenFOAM* is discussed later in the document.) The numerical method is based on the Reynolds Averaged Navier-Stokes equations that describe the flow of a viscous incompressible fluid. The free surface is captured by the Volume of Fluid (VOF) method, while the turbulence closure is based on the $k-\omega$ turbulence model. The solution is calculated using the Finite Volume approach and the PISO algorithm is used to handle pressure-velocity coupling [17]. Fig. 6 demonstrates the visualisation of one of the generated CFD meshes and displays streamlines of the surface flow. Further details on the *OpenFOAM* CFD code and its mathematical treatment of fluid and turbulent simulations are discussed in sections 3 and 4.

This research [10] concludes that the computational model represents accurately the experimental data, but there is still room for improvement on the inter-linking phases between



surface and sewer networks. Even some of the more complex fluid features were able to be replicated in the CFD model. The main areas of agreement between the two incarnations of the simulation were the fluid depths around the manhole and therefore the drainage behaviour. This work is on-going and has some strong connections with the University and as such will be pursued in order to ascertain the modelling best practice for this scenario. This case study is the most similar to the proposed study, as discussed in the following section; however excerpts of the data and modelling practices from each of the previously mentioned studies can be used in order to perfect the macro-scale simulation of the drainage around the *Hydro Filterra* bioretention system.

Fig. 6 – CFD Simulation of Gulley Pot Including Streamlines [10]

The above experimentation and computational approaches are not the only ones that were analysed within this section of the report, for the sake of brevity, however they are the only ones addressed herein. Separate elements of the above papers shall be extruded in order to develop a methodology for the design of this project. This is addressed in the following section as well as further information on the CFD code *OpenFOAM* and the mathematical approaches to solving the project case.

3. Methodology & Mathematical Foundation

Section 3 describes the project trajectory and some detail on the processes adopted to successfully complete this project, based on the previously described research. The project plan, presented in the following section is an abridged version of that submitted in the associated I1 report. Also covered in this portion of the report are some details on the CFD code *OpenFOAM* and the mathematical approach adopted to resolve free surface simulations.

3.1 Project Plan

Continuing from the given research, the following project plan was established in order to achieve the project aims and objectives. These tasks are listed in chronological order:

- Develop a good working knowledge of the mechanics and operation of *OpenFOAM* CFD code.
- Use *OpenFOAM* software to construct simple weir / orifice drainage models and compare these with those examined in the literature in order to achieve validation of the methodology
- Build a 2-dimensional representation of the case study bioretention units based on the information provided by *Hydro International* including the external geometry and taking into account the drainage behaviour prior to the unit inlet
- Construct a 3-dimensional model of the inlet to the case study *Hydro Filtterra* system including the external flows (where relevant) and run optimisation tests on the location and orientation of the unit installation. The 3-dimensional model is important as the UK variation of the bioretention unit feature a series of inlet slots to the kerb as opposed to the single slot US variation on the system
- Construct, with the information from Pavey and Ronald [6 & 7], a full, 3D simulation of the entire *Hydro Filtterra* installation and compare this macro-level simulation in *OpenFOAM* with the SWMM5 generated by Winston-Gore [18] in order to provide some validation to the model. This could also be compared with empirical data available from *Hydro International*.

3.2 Computational Fluid Dynamics & *OpenFOAM*

Computer Aided Engineering (CAE) is becoming increasingly prominent throughout industry as there are clear economic advantages to testing product development in a virtual environment ahead of manufacture. One of the most prominent areas within this field is Computational Fluid Dynamics (CFD). CFD is the process of solving numerous simultaneous equations relating to fluid behaviour and is very mathematically intensive. The process is based on the Navier-Stokes equations which, for an incompressible fluid, can be expressed as:

$$\nabla \cdot \underline{u} = 0 \quad \text{Eq. 1}$$

$$\frac{\partial \underline{u}}{\partial t} + \nabla \cdot \underline{u} \underline{u} = -\frac{1}{\rho} \nabla p + \nu \nabla^2 \underline{u} \quad \text{Eq. 2}$$

Where:

\underline{u} = Velocity (ms^{-1})

t = Time (s)

ρ = Density of Fluid (kgm^{-3})

p = Pressure (Pa) and

ν = Kinematic Viscosity (m^2s^{-1})

Equation 1 is referred to as the continuity equation and is derived from the principle of the conservation of mass and momentum. It states that the fluid is incompressible. The terms from Equation 2 can be rearranged to provide 3 equations with 4 unknowns, resulting in strong coupling and thus it is possible to solve for the case. This is a relatively complex mathematical process, even for a 1D case. Computational processing is therefore essential in simultaneously determining as many parameters of fluid behaviour as possible

Most mathematical models in CFD use a standard transport form for solving unknown quantities (q), as shown below. The virtual domain is divided into small cells in the form of a 'mesh'. The equations are then integrated across the volume and difference equations are produced which can be solved through matrix inversion. This process is known as the Finite Volume Method. The standard transport form is given as:

$$\frac{\partial q}{\partial t} + \nabla \cdot \underline{u}q = \Gamma_q \nabla^2 q + S_q \quad \text{Eq. 3}$$

Where:

q is the quantity to be resolved

$[\nabla \cdot \underline{u}q]$ determines how the quantity moves around the domain

Γ corresponds to the diffusivity of the quantity and

S_q is a source term, dictating whether q is being created or destroyed

This transport equation can be used in software such as *OpenFOAM*, Fluent and many other CFD codes to resolve virtually any desired quantity, be it temperature, volumetric flow rate, or even stock price indicators.

There are many options available to the modeller for implementing CFD on this project case, but the software choice for the present work is *OpenFOAM*. This open source software is available to the user with no license fee and with greater degrees of freedom with regard to case manipulation. For example, it is possible within *OpenFOAM* (to a user with the relevant skill-set) to develop new codes which better handle the simulated case and demands a more complex understanding of the basic physical principles involved in fluid dynamics.

3.3 Mathematical Approach to Free Surface Flow

The following section describes the mathematical foundation of *interFoam*, a commonly used *OpenFOAM* code. This code is used for free surface and multiphase simulations such as those addressed within the present work. It has demonstrated its validity within the literature [10] and shall, along with *porousInterFoam* (a code that also applies porosity values to given regions within the domain), be the main practice in solving the proposed modelling cases.

The *OpenFOAM* application *interFoam* is based on the Pressure Implicit with Splitting of Operators (PISO) algorithm and uses the Eulerian approach known as Volume of Fluid (VOF) method. This algorithm implements a momentum predictor and a correction loop in which a pressure equation based on volumetric continuity equation is solved and the momentum is corrected based on a pressure change. This method uses a fixed mesh, with the two fluids moving through it whose concentration is implied by a phase fraction (α). The fluid is assumed to be Newtonian and incompressible. As such, the governing equations take the following form:

Continuity Equation (as Eq. 1 above):

$$\nabla \cdot \underline{u} = 0 \quad \text{Eq. 1}$$

The momentum equation now is given by:

$$\frac{\partial \rho \underline{u}}{\partial t} + \nabla \cdot (\rho \underline{u} \underline{u}) = -\nabla p + \nabla \cdot \tau + \rho \underline{f} + \sum_{i=1}^N \sum_{k=i+1}^N \underline{F}_{ik} \quad \text{Eq. 4}$$

Where:

τ = viscous stress tensor

\underline{f} = gravitational force and

\underline{F}_{ik} is derived from Gauss' Theorem and is expressed as:

$$\underline{F}_{ik} = \int_{S(t)} \sigma_k \kappa \delta(x - x') dS \quad \text{Eq. 5}$$

Eq. 5 is the influence on the momentum due to the surface tension forces of the interface between phases. In this case, the number of phases (N) is 2. The density (ρ) and viscosity (μ) are expressed as:

$$\rho = \sum_{i=1}^N (\alpha_i \rho_i) \quad \text{Eq. 6}$$

And:

$$\mu = \sum_{i=1}^N (\alpha_i \mu_i) \quad \text{Eq. 7}$$

Where α_i is the volume fraction of the phase i . The transport equation for the i^{th} fraction is therefore:

$$\frac{\partial \alpha_i}{\partial t} + \nabla \cdot (\alpha_i \underline{u}) = 0 \quad \text{Eq. 8}$$

Where the phase fraction (α_i) takes a value of 0 or 1 dependent on whether the fluid is air or water respectively.

A continuum surface force model, developed by Brackbill [19] is also included in the *interFoam* application. Treating the model as such means that the surface tension is interpreted as a continuous, three dimensional effect across an interface. This implicit method is adopted as the shape or location in mesh of the interface is unknown and as a result it is not possible to set a boundary condition. The influence of surface tension (σ_{ik}) is expressed as a volumetric force:

$$F_{ik} = \sigma_{ik} \kappa_{ik} (\nabla \alpha)_{ik} \quad \text{Eq. 9}$$

Where:

$$(\nabla \alpha)_{ik} = \alpha_k \nabla \alpha_i - \alpha_i \nabla \alpha_k \quad \text{Eq. 10}$$

The curvature is defined such that:

$$\kappa_{ik} = \nabla \cdot \left(\frac{(\nabla \alpha)_{ik}}{|(\nabla \alpha)_{ik}|} \right) \quad \text{Eq. 11}$$

And can be written in terms of the normal vector (\underline{n}) as:

$$\kappa_{ik} = -\nabla \cdot \underline{n} \quad \text{Eq. 12}$$

Since the model considers only Newtonian fluids, the stress tensor is given by:

$$\tau = \mu (\nabla \underline{u} + \nabla \underline{u}^T) \quad \text{Eq. 13}$$

The divergence of which can be given by:

$$\nabla \cdot \tau = \nabla \cdot (\mu \nabla \underline{u}) + (\nabla \underline{u} \cdot \nabla \mu) \quad \text{Eq. 14}$$

And the pressure term can be substituted by:

$$p = p^* + \rho \underline{f} \cdot \underline{x} \quad \text{Eq. 15}$$

Resulting in the following equation at the heart of the *interFoam* code (Eq. 16):

$$\frac{\partial \rho \underline{u}}{\partial t} + \nabla \cdot (\rho \underline{u} \underline{u}) = -\nabla p^* + \nabla \cdot (\mu \nabla \underline{u}) + (\nabla \underline{u} \cdot \nabla \mu) - \underline{f} \cdot \underline{x} \nabla \rho + \sum_{i=1}^N \sum_{k=i+1}^N \sigma_{ik} \kappa_{ik} (\nabla \alpha)_{ik}$$

Other influences on the mathematical operation of the *interFoam* application, such as turbulence models and differencing schemes are discussed in later sections of this report.

4. Two-Dimensional Modelling

The following section describes in detail the modelling decisions that were adopted to successfully simulate the drainage case of the *Hydro Filterra* unit in two dimensions. First, the simplification of the inlet geometry is discussed; followed by mesh generation, appropriate boundary conditions and the impact of turbulence modelling. Mesh refinement studies were conducted and subtle design features of the *Hydro Filterra* unit are addressed, namely the influence of the porous region and positioning of the energy dissipating layer at the soil surface. Finally, the results are presented and discussed.

4.1 Initial 2D Inlet Case

Fig. 7, below, is a cross-sectional diagram of the *Hydro Filterra* bioretention system. This was used, along with drawings provided by *Hydro International*, to construct a 2D inlet case.

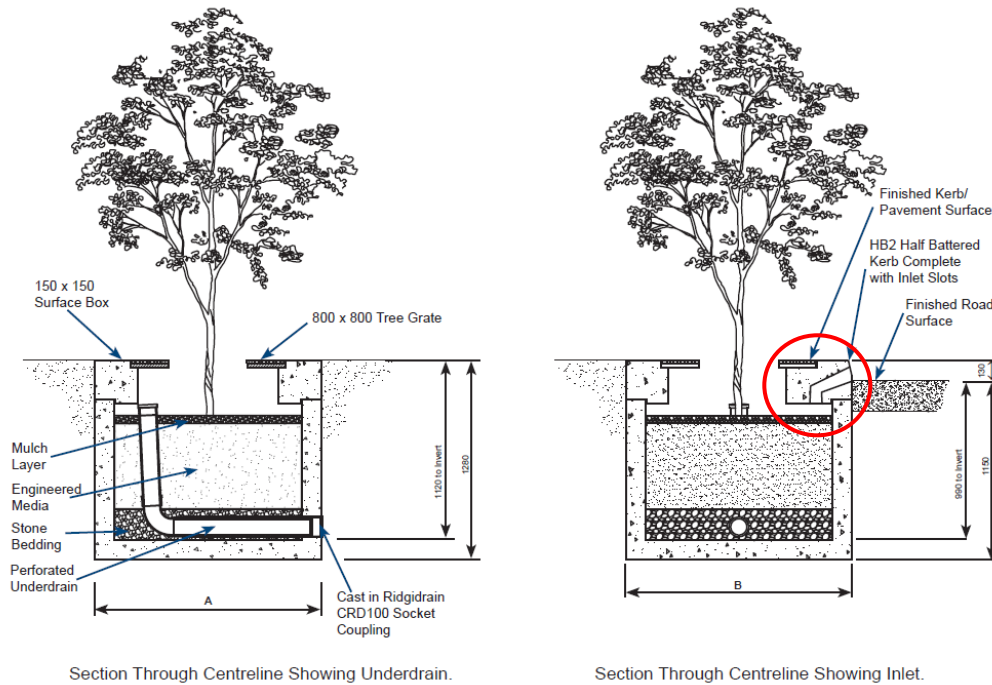


Fig. 7 – Cross-section of the *Hydro Filterra* bioretention unit

4.1.1 2D Inlet Geometry & Mesh Generation

The initial area of focus for the generation of the 2D model was the region circled in red in Fig. 7 above. Fig. 8 displays the geometry that was generated using *blockMesh*, the mesh generation utility in *OpenFOAM*. The *blockMeshDict* files for two simulations, created from scratch, are provided unabridged in Appendices I & II.

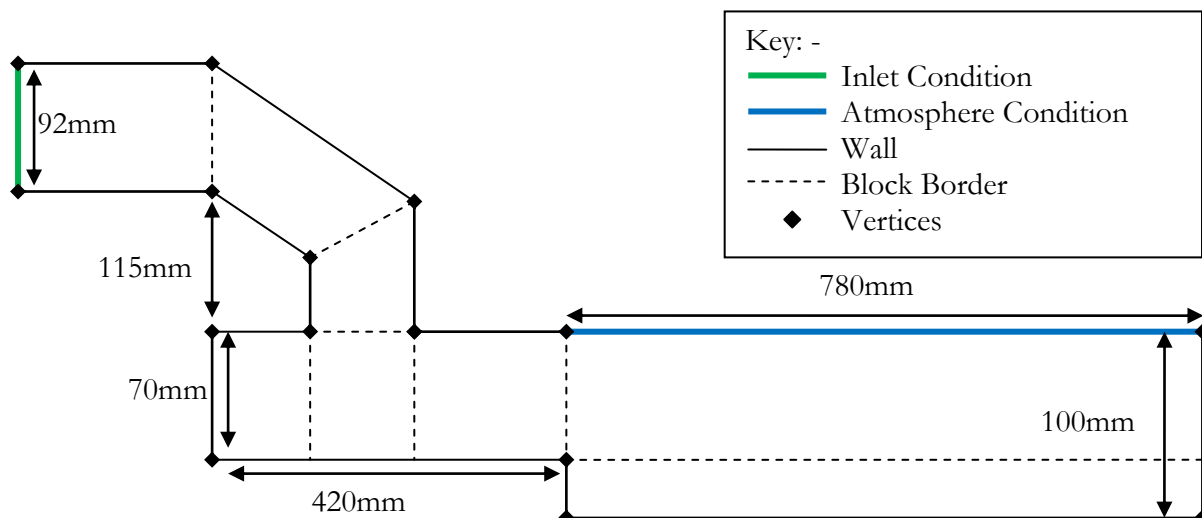


Fig. 8 – Initial 2D Inlet Geometry

The backward facing step, of length 420mm as shown in Fig. 8 represents the energy dissipating layer that sits at the top surface of the soil. Its purpose is to prevent erosion of the soil layers and to regulate and dissipate the incoming fluid flow. This is a portion of the mesh that is augmented in future sections to determine its influence on the operation of the unit. The above geometry was created from scratch in the *blockMeshDict*, where the mesh density is also selected. For the initial case, a cell width of 10mm was selected as this was a simple starting point for mesh refinement and returned good values for the number of cells in each block. Fig. 9 shows the first mesh that was generated for the 2D inlet case.

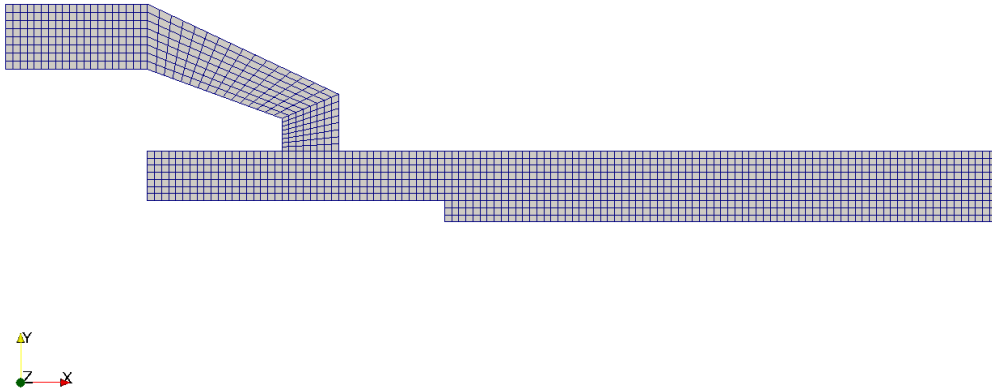


Fig. 9 – First Mesh for Initial 2D Inlet Case

The mesh quality can be verified using the *checkMesh* utility in *OpenFOAM*, which runs a set of very basic quality checks such as skewness and non-orthogonality. The skewness value represents the angle between the line connecting two neighbouring cell centres and the cell face that they share. A low value for skewness is ideal and would indicate line between cell centres that runs perpendicular to the cell face which they share. The non-orthogonality is effectively the straightness of a cell. A regular cuboid would be very orthogonal. Like skewness, a low value is required for a good quality mesh, as this would simplify transport equations between cells.

4.1.2 Boundary Conditions

The next task in building the 2D simulation was then to select appropriate boundary conditions that reflected the physical properties of the case. The first phase of any simulation with regards to its boundary conditions is to determine the Reynolds Number for the flow, given by:

$$Re = \frac{VL}{\nu} \quad \text{Eq. 17}$$

Where:

Re = Reynolds Number (dimensionless)

V = Inlet Velocity (ms^{-1})

L = Characteristic Inlet Length (m)

ν = Kinematic Viscosity (m^2s^{-1})

The velocity is obtained from rainfall data for the installation region, obtained from *Hydro International* [20], collated from the Met Office Deluge Database. Maximum unit capability is also described in this data.

This yielded a volumetric flow rate (Q) of $6.94 \times 10^{-4} \text{ m}^3 \text{ s}^{-1}$ for a maximum rainfall condition. Using Eq. 18 (below) as is known from fluid dynamics, it was possible to determine the velocity based on the wetted area of a single inlet to the unit.

$$Q = VA \quad \text{Eq. 18}$$

Where:

Q = Volumetric Flow Rate ($\text{m}^3 \text{ s}^{-1}$)

V = Velocity (ms^{-1})

A = Area (m^2)

Given a water depth of 35mm [10], and the width of a single inlet channel on the *Hydro Filterra* unit of 124mm [21], this yielded an inlet velocity for a peak flow condition of 0.1599 ms^{-1} .

The characteristic length (L) was determined using the hydraulic diameter, a ratio used in channel flow [16, 22] that relates the area of the inlet cross-section to the wetted perimeter of the channel such that:

$$D_H = \frac{4A}{P} \quad \text{Eq. 19}$$

Where:

D_H = Hydraulic Diameter (m)

A = Cross-sectional Inlet Area (m^2)

P = Wetted Perimeter of the Channel (m)

In the given case, hydraulic diameter was calculated as 0.235m. The resultant Reynolds Number for the case at maximum inflow for water at normal atmospheric conditions is therefore calculated as:

$$Re = \frac{0.1599 \times 0.235}{10^{-6}} = 37,611$$

In order to maintain a constant flow rate and water depth at the inlet, it was necessary to apply an inlet boundary condition using *groovyBC*. This utility allows the user to apply various styles of inlet conditions, such as turbulent, parabolic and position-dependent conditions. For this case, the *groovyBC* entry for the phase fraction (*alpha1*) at the inlet was given by:

```
inflow
{
    type                groovyBC;
    variables            "surface=0.22;";
    valueExpression      "(pos ().y <= surface) ? 1.0 : 0";
    value                uniform 1;
}
```

The above entry states the *inflow* condition as *groovyBC*, calling the appropriate library for this function. The variable *surface* is tested against the *valueExpression* equation to determine whether a point on the *inflow* face is above or below the water level. For this case, the water level is 0.22m, corresponding to a water depth of 35mm when considered using global positioning coordinates.

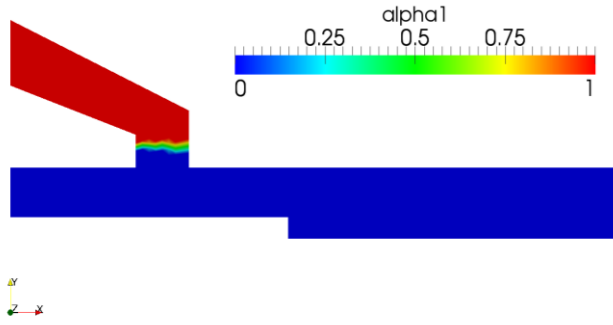


Fig. 10 – *Alpha1* Field for Initial 2D Inlet

A further boundary condition can be set for the *alpha1* field such that a particular region of the domain is initially a wholly water phase. This is affected by the *setFields* utility in the */system* folder. In the first test cases of the 2D simulation, the inlet region was set to water phase, as illustrated in Fig. 10, but this was deemed unphysical as at the 0th time-step, the wall of water flushed through the system and is not representative, even in flood conditions, of the fluid behaviour. Alpha1 = 1 represents water and alpha1 = 0, air.

The final two initial conditions to set in this case relate to the turbulence model selection. These are the turbulent kinetic energy (k) and its rate of dissipation (ϵ). These can be derived from knowledge of the Reynolds Number and inlet velocity as previously calculated such that [23]:

$$k = \frac{2}{3} (U_{ref} T_i)^2 \quad \text{Eq. 20}$$

Where:

k = Turbulent Kinetic Energy (m^2s^{-2})

U_{ref} = Inlet Velocity (ms^{-1})

T_i = Turbulence Intensity (dimensionless) and is defined as [24]:

$$T_i = 0.16 Re^{-1/8} \quad \text{Eq. 21}$$

The dissipation of Turbulent Kinetic Energy (ϵ) is given by:

$$\epsilon = C_\mu^{\frac{3}{4}} \frac{k^{\frac{3}{2}}}{l} \quad \text{Eq. 22}$$

Where:

$l = 0.07L$

And:

L = Characteristic Length Scale (m)

C_μ = Turbulent Kinetic Energy Coefficient (dimensionless)

ϵ = Dissipation of Turbulent Kinetic Energy (m^2s^{-3})

From the above equations, values for k and ϵ were determined as 3.13×10^{-5} and 1.752×10^{-6} respectively. Standard *epsilonWallFunctions* were applied to the wall boundary conditions for ϵ and the inlet was given a fixed value. The wall boundaries were given standard *kqRWallFunctions* for k and again the inlet was given a fixed value inlet.

4.1.3 Applying Different Turbulence Models

The standard k- ϵ turbulence model is generally accepted as the default industry standard, but there are a number of different models which are available with some minor alterations in the case file. The following sections describe a few of the turbulence options available with *OpenFOAM*:

- RNG k- ϵ Model

This model takes into account smaller scales of motion through re-normalisation of the Navier-Stokes equation. The standard k- ϵ model is somewhat restricted by only accommodating a single turbulent length scale to model the eddy viscosity. The RNG approach however recognises that turbulent diffusion occurs within all scales of motion and accounts for this through changes to the production term. Applying this model required alteration to the k and ϵ files in the *0/* directory as well as selection of the relevant (*RNGkEpsilon*) option in *RASProperties* and *turbulenceProperties* dictionaries.

- k- ω SST Model

The k- ω SST model is a two-equation eddy-viscosity model using the shear stress transport (SST) formulation, meaning it uses two extra transport equations to represent the turbulent properties of the flow. This allows a two equation model to account for history effects like convection and diffusion of turbulent energy, providing more accuracy closer to the wall through the viscous sub layer and as such can therefore be used as a low Reynolds Number turbulence model without extra damping functions. The SST model also adopts behaviour similar to that of the k- ϵ model in the free stream and as such is more robust than the standard k- ω model. Its implementation is similar to that of the k- ϵ model and can be invoked in a manner similar to that of the RNG k- ϵ model. The ω term is the specific dissipation and determines the scale of the turbulence. Its value is calculated from k and ϵ applied in Eq. 23. The units for ω are s^{-1} . [25]:

$$\omega = \epsilon/k \quad \text{Eq. 23}$$

- Launder-Reece-Rodi (LRR) Reynolds Stress Model

The LRR Reynolds Stress Model is a far more sophisticated turbulence model. Instead of calculations being based on the eddy viscosity, a field for the Reynolds stress tensor is required and invoked using the *R* utility. Implementation is similar to the other models, changing the entry in *RASProperties* and *turbulenceProperties* dictionaries. Computation of the Reynolds stress tensor is based on the initial quantities of k and ϵ as described above.

Four different turbulence models were simulated in order to observe any dramatic effects on physical behaviour. These included standard k- ϵ , RNGk- ϵ , standard k- ω and k- ω SST. Since there was no empirical data to validate each simulation, selection of the appropriate turbulence model was decided through historical evidence in the literature [10, 12, 13], indicating that k- ω SST was the best candidate. Its advantages include:

- Greater numerical stability, due to absence of damping functions
- More accurate near-wall treatment as well as free stream velocities
- Has been shown through the literature that it provides an accurate analogue for urban drainage cases

4.1.4 Mesh Refinement

A good quality mesh is necessary for a successful simulation. There is however a trade-off between quality and computational expense. Furthermore, depending on the required analysis, there will be a point where the simulation achieves mesh independence i.e. refinement of the mesh until there is no change in the final values of the required field. A mesh refinement study is therefore required to establish if this can be achieved for the present simulation.

From the initial mesh, as described by Fig. 9, an arbitrary ‘growth factor’ of 1.3 was applied to each of the block cell-counts in the *blockMeshDict* in the x- and y-directions. The depth z was retained as 1 cell to limit the calculation to a 2D mesh. A total of 5 new meshes were generated and their quality evaluated using *checkMesh*. The mesh accuracy was judged visually by definition / clarity of the *alpha1* field and the U_y field was also evaluated at the final time-step $t=5s$ in each case to check convergence. A total of 6 meshes were generated and are summarised in Table 1, beneath Fig. 11 which gives examples of the visual mesh quality and difference in mesh density.

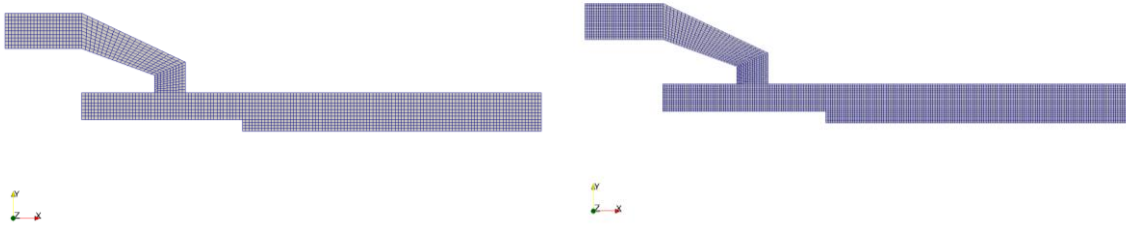


Fig. 11 – Mesh Refinement Process

Table 1 – Mesh Refinement Table

Mesh Number	Number of Cells	Minimum U_y Value (ms^{-1})	Clocktime (s)
0	1426	-1.921	111
1	2066	-1.861	156
2	3083	-1.486	255
3	4414	-1.388	456
4	6250	-1.419	808
5	8877	-1.423	1473

The selection of U_y as the convergence criteria is somewhat arbitrary, but this is also a quantity prominent in a region of the computational domain (Fig. 12) which is dominated by gravitational effects. It therefore has some independence from other fluid behaviours and physical effects. Another factor that was judged in the mesh refinement process was the definition of the *alpha1* field. Since the aims of the project are to observe the fluid behaviour, it is important to visualise the clarity of the water-phase and its movement within the domain. Fig. 13 demonstrates the difference between two mesh densities in this manner. It was decided from the mesh refinement study that for the 2-dimensional cases, mesh 3 was most suitable as it supplied sufficient accuracy as well as being relatively computationally inexpensive, a trait that will be significant in the move to 3-dimensional analysis.

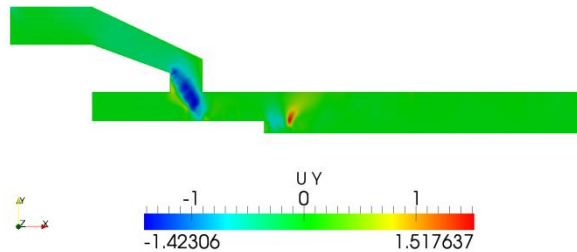


Fig. 12 – U_y Velocity Field for Mesh Refinement 5

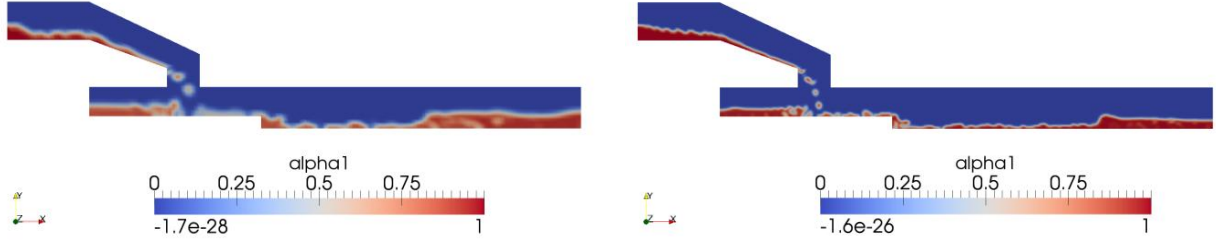


Fig. 13 – *Alpha1* Field for mesh Refinement 1 (left) and 5 (right)

4.2 The Addition of a Porous Zone

The *OpenFOAM* application *porousInterFoam* is similar to the previously described *interFoam* code but includes an additional, augmented pressure-drop term at the end of the Navier-Stokes Equations. This additional term is a resultant of the Darcy-Forchheimer Law and is dependent on the volume fraction of the porous media and the average particle diameter. The volume fraction was obtained through the work of Begley [26] using *ScanIP* software to transform CT scans of the media into computational meshes. The average particle diameter was obtained from sieve tests and rapid prototyping by Please [27]. The *porousInterFoam* application has been validated and discussed in greater detail by the work of Pavey [6]. Experimental and computational analysis has shown very good agreement for this case.

The additional dictionary *porousZones* is required in the */constant* folder in order for *porousInterFoam* to run. An excerpt from this dictionary is given below:

```
Darcy
{
    d      d[0 -2 0 0 0 0 0] (1.42e9 1.42e9 1.42e9);
    f      f[0 -1 0 0 0 0 0] (9.86e4 9.86e4 9.86e4);
}
```

This entry selects the Darcy-Forchheimer system and the values for d and f , which are derived from the following equations:

$$d = \frac{150}{d_p^2} \cdot \frac{(1 - \epsilon)^2}{\epsilon^3} \quad \text{Eq. 24}$$

And:

$$f = \frac{3.5}{d_p} \cdot \frac{(1 - \epsilon)}{\epsilon^3} \quad \text{Eq. 25}$$

Where:

d_p = Average Particle Diameter (m)

V_{air} = Volume of Air (m^3)

V_{Total} = Total Volume of Sample (m^3)

ϵ = Volume Fraction (dimensionless) and is given by:

$$\epsilon = \frac{V_{\text{air}}}{V_{\text{Total}}} \quad \text{Eq. 26}$$

4.3 The Influence of the Energy Dissipation Layer

Inclusion to the 2D model of the *porousInterFoam* application allows for greater detail on the inlet flow behaviour as a whole and facilitates analysis of the energy dissipating stones at the surface of the soil. These have been included to disperse the flow across a broader portion of the soil surface and to limit erosion from the run-off at the inlet. It is necessary to determine the impact of the stone on the fluid dissipation within the domain and the drainage into the porous media.

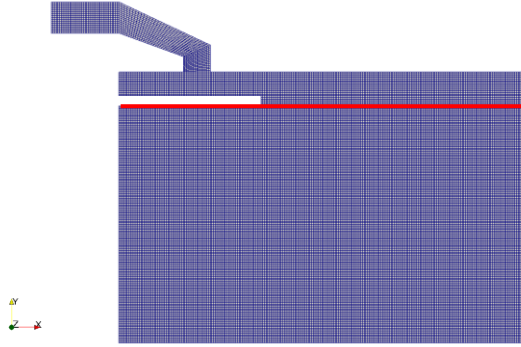


Fig. 14 – Original Inlet with Porous Zones

In order to achieve this, the *blockMesh* dictionary had to be expanded to include additional blocks that could be given porous properties as outlined in the previous section. Three examples of slab design were evaluated to establish which was most appropriate for the case. Figs. 14 & 15 show the energy dissipating stone options that it was possible to construct using *blockMesh*.

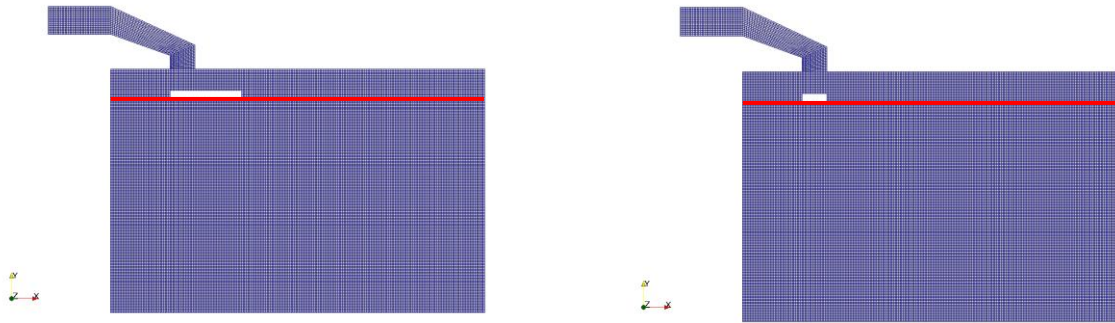


Fig. 15 – Slab Options 1 (left) and 2 (right)

In the images above, the white portion within the internal domain represents the energy dissipating stone. Working at the limit of the capabilities of *blockMesh* and project time constraints, it was only possible to generate two variations on the original, which is depicted in Fig. 14. The same inlet boundary conditions as described in section 4.1.2 are maintained and no additional outlet faces are specified. The area vertically beneath the energy dissipating layer, indicated by the red line in the above images, is the porous region and adopts the properties as described in the previous section. Fig. 16 is a representative image of the fluid behaviour and associated velocities without the additional porous zones and as such, it displays the fluid behaviour if the soil surface were solid where $\alpha_{water}=1$ is the water phase. The colour and size of the arrows represent their respective velocity magnitudes as shown in the colour bar.

The more important factor to establish, however, is how this behaviour changes with the addition of the porous zones and with further changes to the energy dissipating layer. These elements are observed in Figs. 17-19.

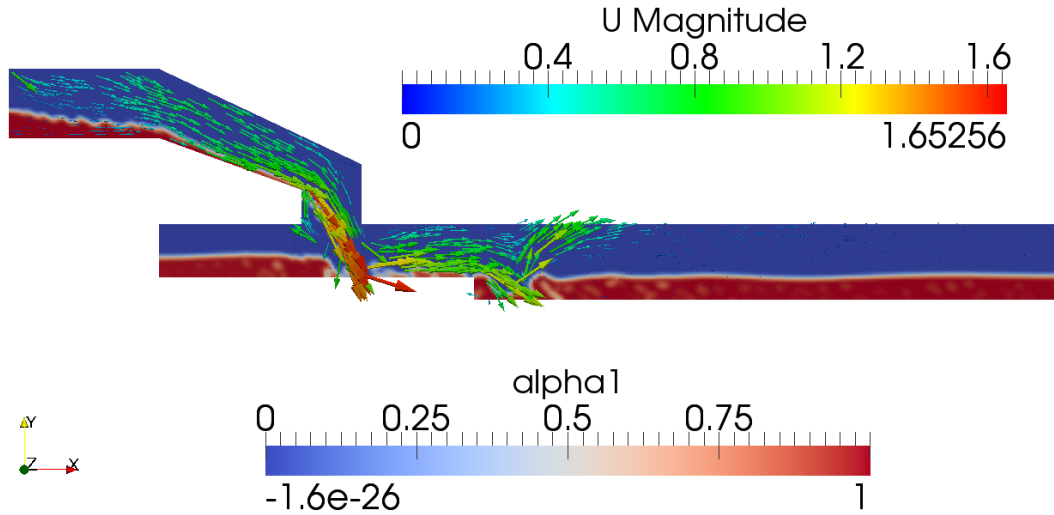


Fig. 16 – *Alpha1* & *U Magnitude* Plot for Initial 2D Model

Fig. 17 below shows how this behaviour changes with time and with the additional porous zones beneath the energy dissipating layer. Time-steps for $t=2$, 4, 7 and 10s are displayed.

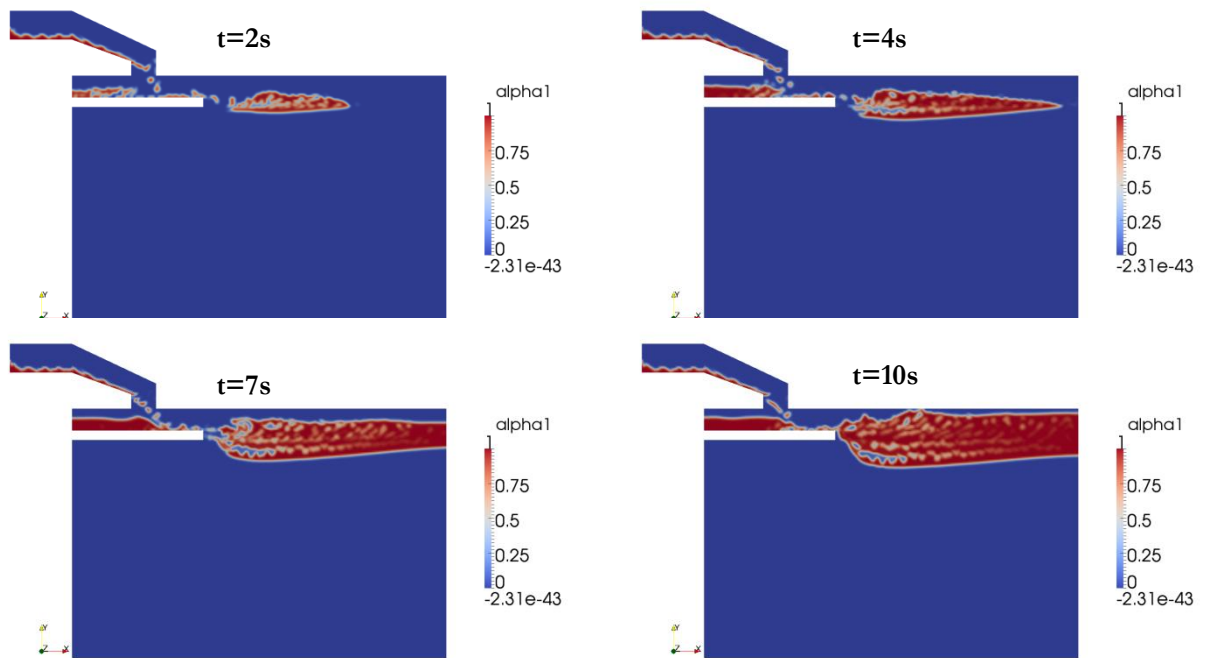


Fig. 17 – Development of *Alpha1* Field in Porous Zones for Original Design.

As can be seen from the above figure, the saturated region of the porous domain evolves in a physically typical manner. The porous blocks provide resistance to the fluid flow, but do not impede it entirely. The simulation is modelled in a ‘worst-case scenario’ where a flood event has occurred after a long dry spell and as such, the porous region is modelled as initially entirely unsaturated and the large influx of water changes these conditions rapidly. At present, there is no application such as *groovyBC* to accommodate a transient porous resistance that would be generated by an increased saturation and so the above model is the most accurate analogue available. Fig. 18, on the following page presents the same case, but for an alternative slab design.

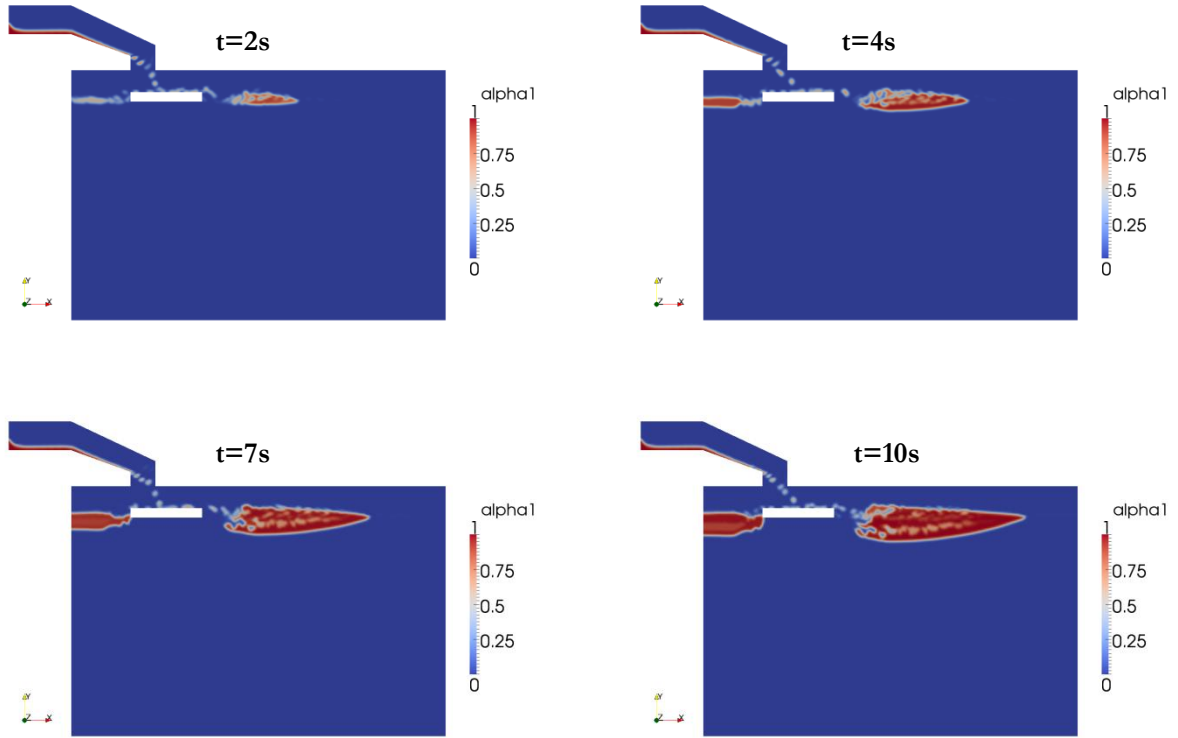


Fig. 18 – α_1 Field Progression for Slab Variation 1

Despite having precisely the same simulation characteristics as the original design, other than the width of the slab, there appears in this model to be a significant difference in the development of the α_1 field. Drainage is handled a lot better in this variation as water is allowed to drain from both ends of the energy dissipating layer.

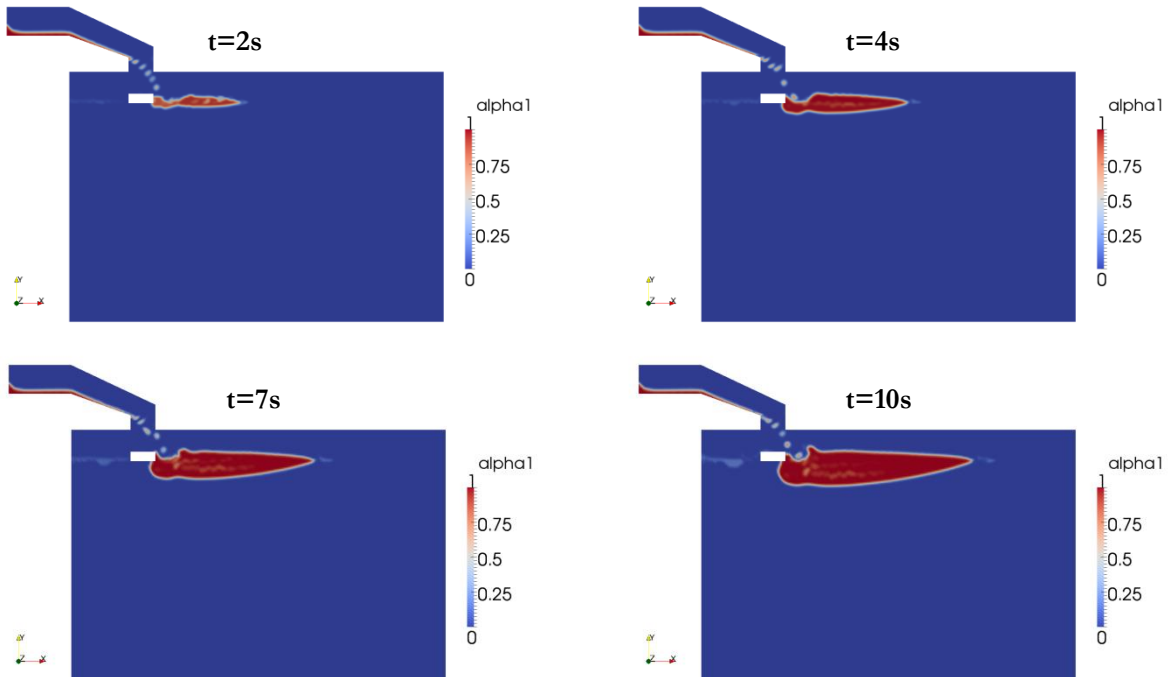


Fig. 19 – α_1 Field Propagation in Slab Variation 2

Fig. 19 shows the same data as the previous two cases for the second variation on the width of the energy dissipating layer. Table 2 displays the differences in water depth above the soil surface, the drainage depth and the total drainage width for each slab variation. The measurements were taken using the *Plot over Line* function available in *ParaView*, the visualisation software associated with *OpenFOAM* from which all the previous images have been taken. These data are accurate to within 5mm, as defined by the mesh resolution.

Table 2 – Energy Dissipation Layer Design Comparison Table

Slab Variation	Max Water Depth	Max Drainage Width	Drainage Depth
Original	80mm	700mm	85mm
Variation 1	35mm	625mm	75mm
Variation 2	25mm	565mm	80mm

As can be seen from the above table, each slab variation has its own advantages and disadvantages. The original case shows better depth of drainage, but also significantly larger depth above the soil surface. The second variation has the best performance overall, but fluid flow is now directly onto the soil surface, which would result in erosion.

4.4 Summary & Discussion of 2D Modelling

Appropriate boundary conditions have been implemented, derived from rainfall data and geometrical configurations applicable to the case study in Barry. These have delivered a reasonable analogue for phase field propagation using the VOF method as implemented by *porousInterFoam* applicable to the case study example of the *Hydro Filterra* unit.

In the validation by Pavey [6] of the *porousInterFoam* code, reference is made to the use of Particle Tracking Velocimetry (PTV) in experimental analysis by Lee [28]. In his work, Lee used PTV to measure fluid velocity in the vicinity of a porous fence. PTV is an optical experimental method used to measure the velocity of fluid particles in a given field. For the present case, however, PTV is not a suitable method of experimental analysis as it relies on tracking small particles using lasers, which would not be possible for the large fluid volumes in a porous zone. Other techniques such as hot-wire anemometry (HWA) and Laser Doppler Anemometry (LDA) would also be insufficient methods of analysis as they do not provide information on the instantaneous spatial structure of the flow. Delnoij [29] discusses radioactive particle tracking where the local displacement of a marker particle is traced and its velocity computed from that information. Again, this will not provide information on the fluid phase fraction, but is a more suitable method of measuring velocity. A straight-forward method of observing the phase fraction progression would be to reconstruct the unit in a laboratory environment with Perspex or other clear plastic walls bounding the soil. Digital Image Correlation (DIC) could then be used to directly observe the fluid flow volumetrically and this series of images could be used to validate the computational data.

The influence of the energy dissipating stone has also been investigated at this level and it has been observed that allowing for run-off at both ends of the stone will result in better drainage behaviour. Since the exact geometry of this element was not available and restrictions in the *blockMeshDict* impede accurate analysis, a cost-benefit analysis was not possible. It is clearly seen, however, the importance of the energy dissipating layer and its effect on the unit. Experimental investigations could be conducted to determine the range of trajectories for different flow rates from the inlet drain onto the soil. These could then be used to establish the optimum width of the slab.

5. Three-Dimensional Modelling

Once the inlet conditions had been modelled in two dimensions, the process of creating a full-scale 3D model of the entire system was then planned in 3 steps, the first two of which are addressed in the present section:

- Expand previous 2D Inlet case to include cells in the z-direction – this will ensure that continuity between 2D and 3D modelling principles are conserved and will verify if the same practices can be adopted with regard to boundary conditions
- Extend *blockMeshDict* to include 3 further blocks representing the car park so that a cross-flow model can be developed with one drain inlet to the model – this will establish any additional boundary conditions that are necessary to replicate a draining car park
- Collaborate to produce a full 3D model with the inlet boundary conditions as established in the present work as well as the porous behaviour and root architecture elements

5.1 3D Inlet Case Simulation

The first phase in developing a 3D model of the *Hydro Filterra* system was to add cells in the z-direction of the *blockMesh* dictionary from the 2D case. This initial step was included to ensure that the 2D model was a valid simplification of the inlet and to establish any adverse effects that arise from 3D modelling, for example flow velocity interference. Fig. 20 demonstrates that the 3D fields match those of their 2D counterparts for the relevant time-steps. The conclusion can therefore be drawn that the 2D representations are an accurate analogue and could be used in analysis to save computational cost.

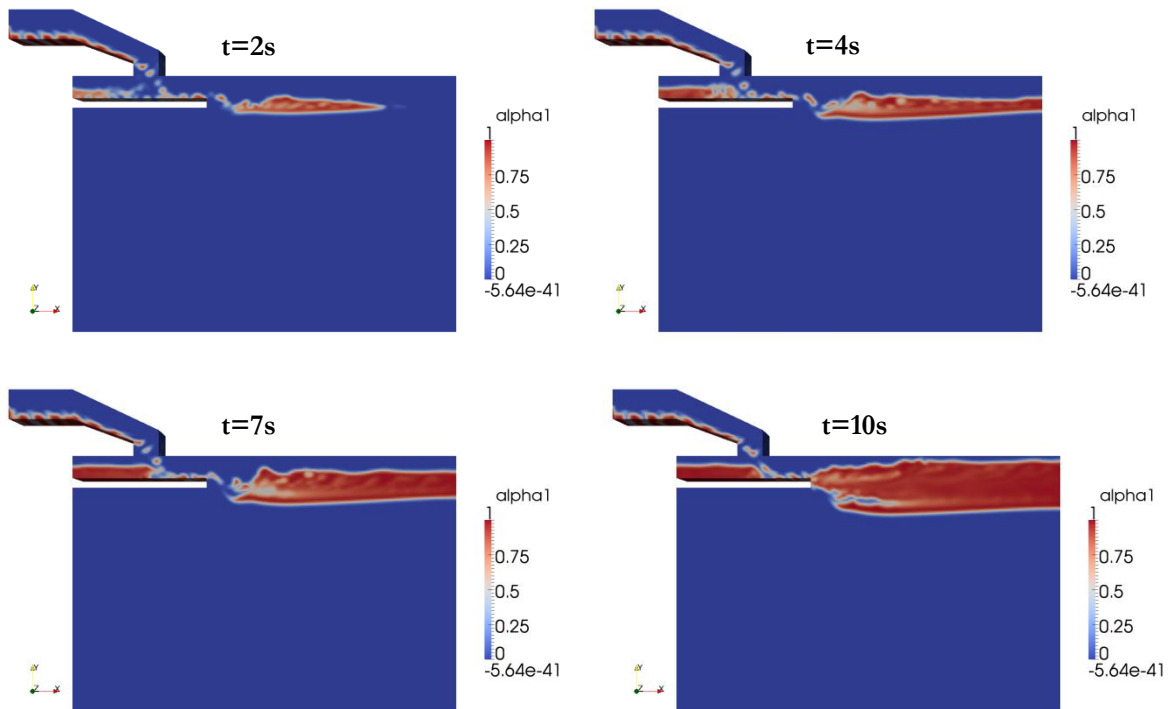


Fig. 20 – *Alpha1* Field For 3-Dimensional Case

5.2 3D Cross-Flow Case Simulation

The second phase to a complete model was to determine the additional input and boundary condition requirements for a 3D case that simulates flow across the face of the drain inlet. Additional blocks were added to the *blockMesh* dictionary to facilitate this. The augmented *blockMeshDict* can be found in Appendix II. Fig. 21 displays the mesh generated for this purpose. The broad street-level region toward the top left of the figure has been constructed with a 1:35 slope towards the curb to replicate the conditions at Barry. This same gradient is present parallel with the curb and has been accommodated by changes to the gravity (*g*) file in the boundary conditions.

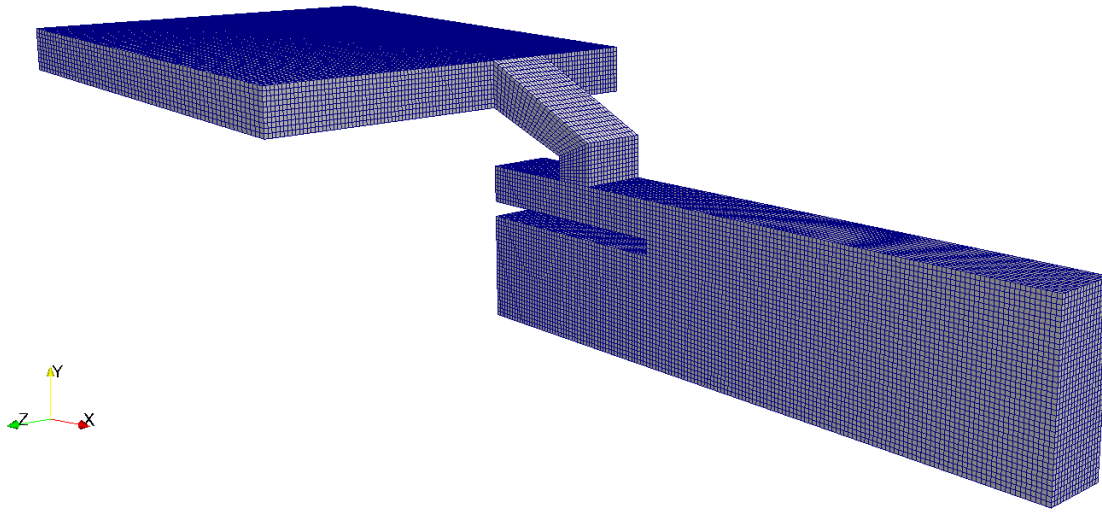


Fig. 21 – Mesh for 3D Cross-Flow Case Simulation

The boundary conditions had to be changed in accordance with equations 17-23 due to the new inlet location. The same rainfall data and maximum inlet condition was used in the calculations, but since the inlet upstream of the drain had increased 4-fold, the flow rate had to be adjusted accordingly.

The upgrade from the simplified inlet condition to a cross-flow simulation proved very difficult as a number of considerations had to be made, such as the change in flow rate and how this affects the turbulence model. A total in excess of 20 modelling approaches were adopted to resolve this modelling scenario, based around different variations of the boundary conditions and the most appropriate analogue selected. The details of the most physically accurate case, selected for use in the present work is described in Table 3, obvious alteration such as case geometry have been excluded for brevity:

Table 3 – Boundary Condition Changes for 3D Cross-Flow Case

Boundary Condition	Change	Reason For Change
setFieldsDict	Include velocity U in setFields	Encourage flow towards inlet
Velocity (U)	$U = (0, 0, -1.262)\text{ms}^{-1}$	Increased Flow Rate
TKE (k)	1.165×10^{-3}	Change in Velocity
Rate of Dissipation (ω)	0.341	Change in Velocity
Gravity (g)	$(0, -9.780, -0.208)\text{ms}^{-2}$	Replicate location topography

The adjusted value for gravity was calculated using trigonometry based on the 1:35 gradient running parallel with the curb on which the unit has been installed. The negative value in the z -direction indicates flow is from the inlet towards the drain. The velocity U was added to the *setFields* dictionary so that the initial water phase would be in motion at the start of the simulation. An outlet condition was also implemented downstream of the drain inlet to allow for fluid to leave the domain.

Although the above constraints were applied to the 3D simulation, the case did not behave precisely as intended with regard to flow across the face of the drain inlet, instead a comprehensive analogue of a car park draining was generated. Given the time constraints of the project as a whole and the number of modelling approaches that were adopted to tackle this simulation problem, a compromise was agreed that the present simulation represented a sufficiently accurate analogue for the drainage case. These input characteristics will be carried forward to the development of the full 3D simulation as discussed in section 6. Fig. 22 is a slice from the internal domain of the case to demonstrate the application of *setFields* for the α_1 and velocity (U) boundary conditions.

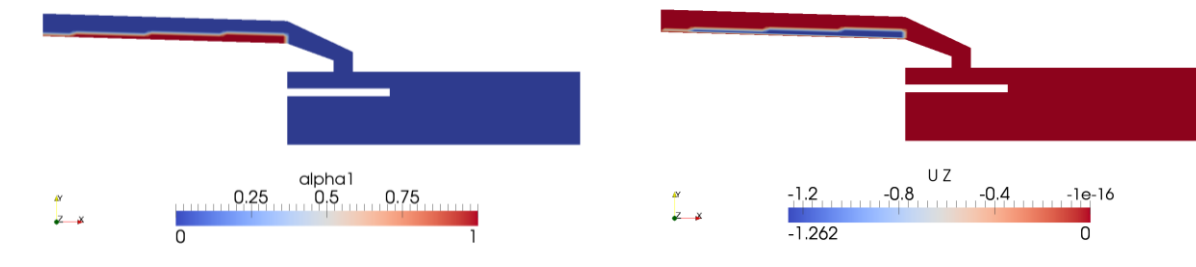


Fig. 22 – Boundary Condition for α_1 (left) and Velocity U_z (right)

Fig. 23 displays the same slice at the first written time-step $t=0.05s$, where the velocity field has completely changed as U_x becomes dominant due to the gradient of the mesh and the simulation attempts to return to equilibrium. The same case was run for a much smaller time-step and it was found that this physical effect occurs as early as $t=0.001s$. This is the effect which is governing the difference between draining the car park region and fluid flow across the face of the inlet. To change the values in order to generate cross-flow would render the simulation un-physical.

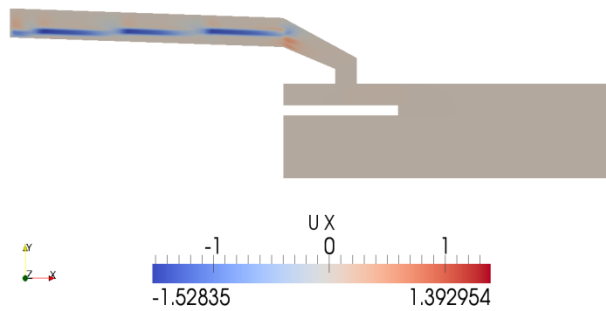


Fig. 23 – U_x Field at $t=0.05s$

Fig. 24 displays the progression of the α_1 field for the time-steps $t=2, 4, 6$ and $8s$. It can be seen that, for the initial stages of drainage, the water level over the drain inlet is the same height as that of the 2D model. Verification of this was achieved through use of the *Plot over Line* function in ParaView. As the car park region drains, however, the flow rate decreases and drainage appears confined to the channel immediately adjacent to the drain inlet in the x -axis. This effect is further visualised in Fig. 25, which displays the same field propagation, but from the underside of the simulation so that the positive y -axis is into the page. Fig. 26 displays the α_1 field for a slice parallel to the x -axis, showing the fluid behaviour adjacent to the drain inlet. Displayed in Fig. 27 is the α_1 field at time $t=5s$ demonstrating the global fluid behaviour.

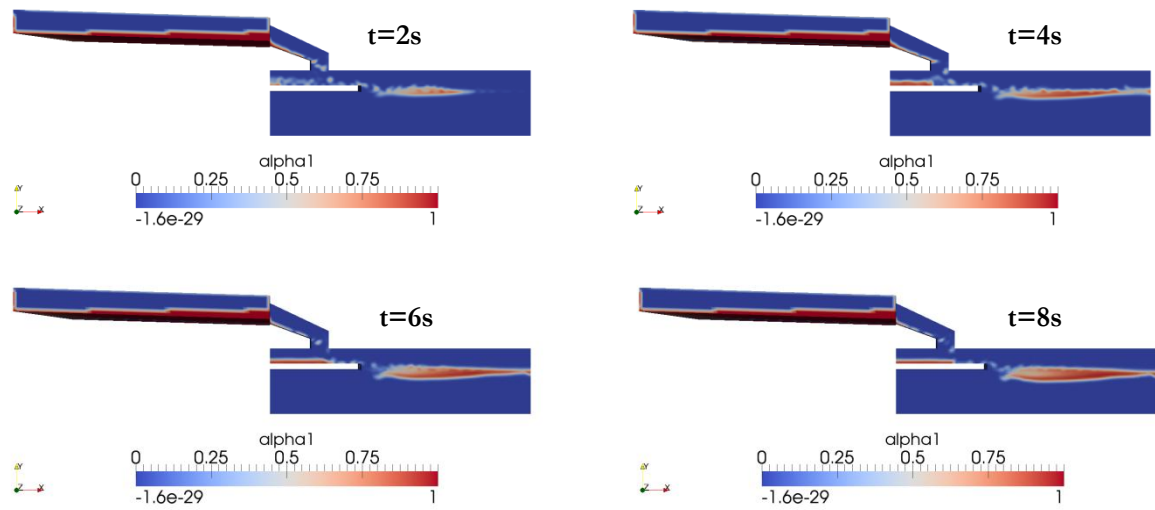


Fig. 24 – α_1 Field Progression in 3D with Street Drainage

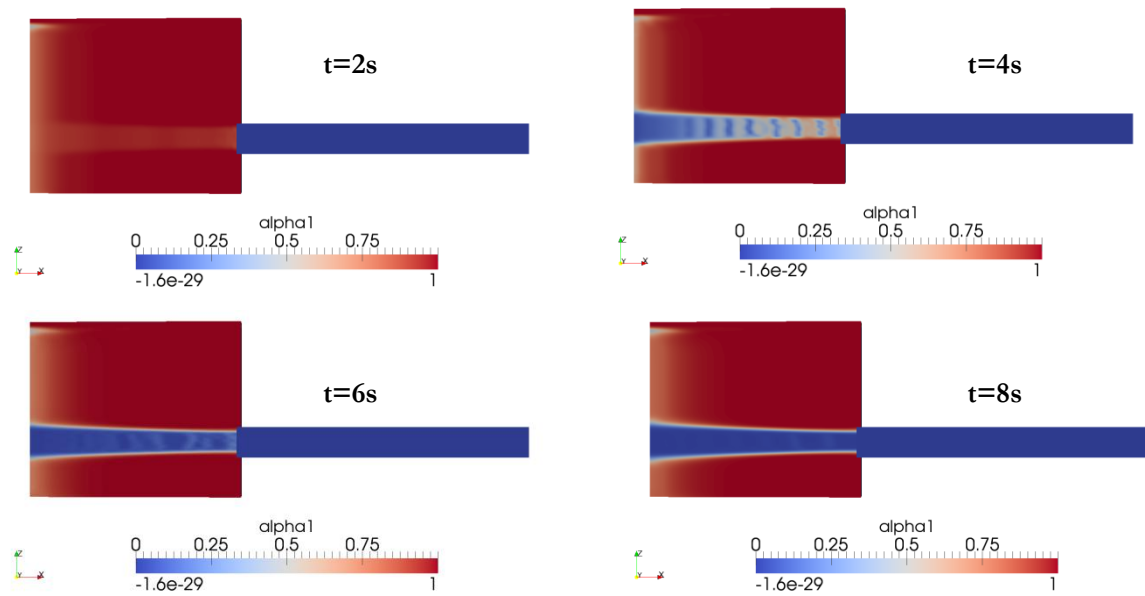


Fig. 25 – View of α_1 Field from beneath Simulated Domain

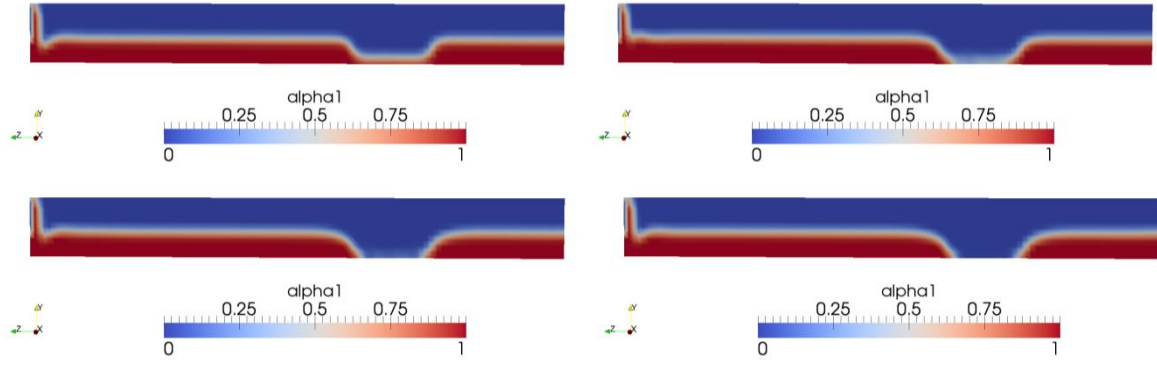


Fig. 26 – α_{11} Field Adjacent to Drain Inlet Clockwise (from top left) $t=2, 4, 8$ and $6s$.

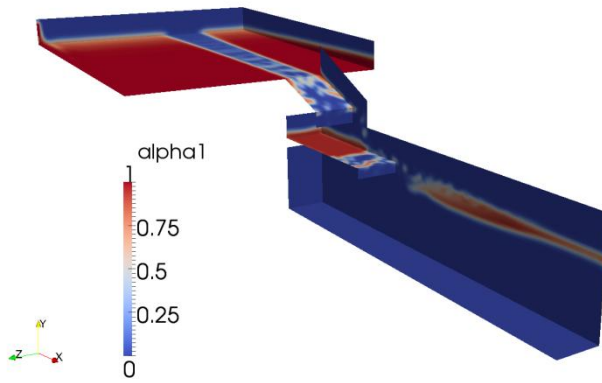


Fig. 27 – Global Position of α_{11} Field at Time $t=5s$

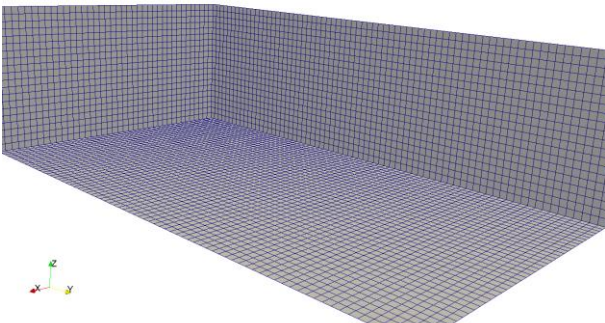
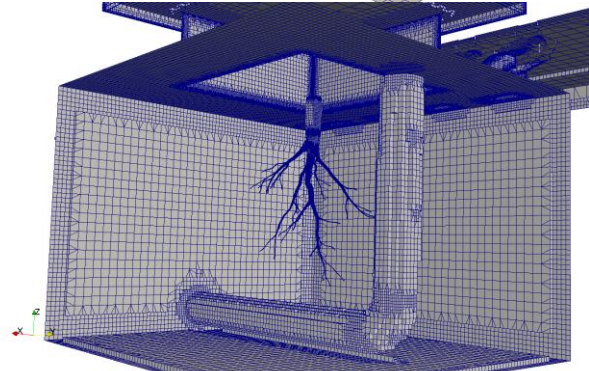
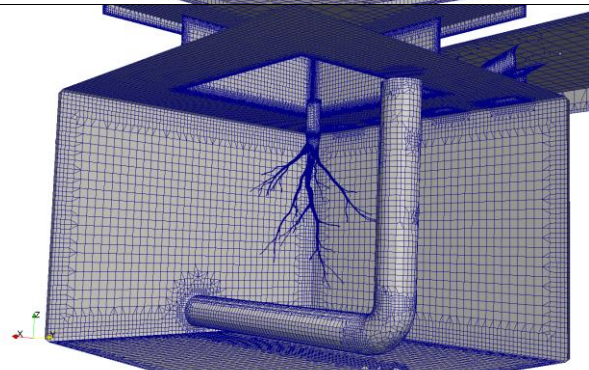
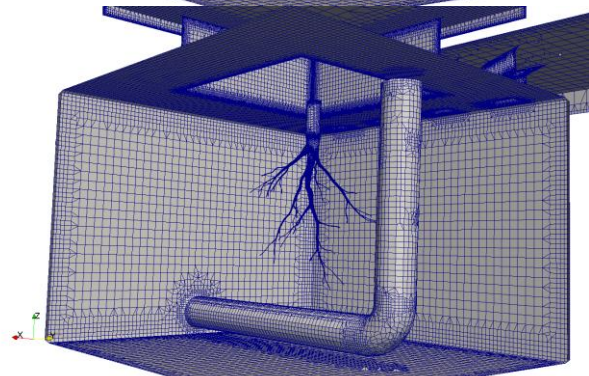
From the above figures, it can clearly be seen that a reasonable analogue for the drainage behaviour of a flooded car park can be simulated using the present mesh and with the boundary conditions as described. These methods can be implemented in the construction of the full 3D simulation, which is discussed in section 6.

6. Collaborative Work & Final 3D Simulation

The following section details the collaborative work undertaken by Pavey, Ronald and Tarrant to construct a full 3D simulation of the *Hydro Filterra* bioretention unit as installed in Barry, South Wales. Accurate modelling geometry for the unit size, car park gradient & unit orientation has been achieved from drawings supplied by *Hydro International* [21]. Inlet conditions as described in the present work have been accepted as suitable analogues for the drainage behaviour in the region immediately adjacent to the unit. Porous regions and the influence of root structures on the system have been adopted from the work of Pavey and Ronald respectively. Individually, each component of the 3D model has been shown to function well and to deliver good results. The inlet conditions have also been combined with the porous zones in the present work and have been shown to provide a sufficient analogue for the 3D case. The root structures have also been investigated individually and have shown good correlation with expected results [7]. This part of the investigation is concerned with the amalgamation of these three factors to determine whether it is possible to generate a full scale model of the installation unit.

In order to progress in 3D modelling of the whole system, a new approach had to be adopted towards meshing the case. The *snappyHexMesh* utility is a meshing tool available in *OpenFOAM*, which allows for more complex shapes to be meshed. This CAD-based meshing tool is controlled by the geometry defined in the .stl files of the objects to be meshed. For this case, a total of 10 .stl files were required to fully define the geometry of all the constituent parts of the model. The *snappyHexMesh* method is outlined in Table 4, below, with representative images of each of the meshing phases.

Table 4 – *SnappyHexMesh* Process

Description of Meshing Phase	Representative Image
<p>Phase 1 – Initial <i>blockMesh</i></p> <p>The first action in using <i>snappyHexMesh</i> is to generate a regular mesh, defined by entries in the <i>blockMeshDict</i> dictionary and as such is not strictly part of the <i>snappyHexMesh</i> process, but is fundamental to its usage.</p>	
<p>Phase 2 – Refinement & Truncation</p> <p>The next generation in creating the mesh is to refine the mesh near the .stl surfaces and to truncate the cells that lie within the boundary. The code ‘knows’ which points lie in the inside and outside of the boundary by the <i>locationInMesh</i> vector, defined in the <i>snappyHexMesh</i> dictionary</p>	
<p>Phase 3 – Snap</p> <p>After the general shape of the object is established, the domain cells directly bordering the .stl objects are ‘snapped’ to the object surface, creating a well-defined, smooth mesh.</p>	
<p>Phase 4 – Add layers</p> <p>This final stage is optional and controlled in the <i>snappyHexMeshDict</i>. In some cases, snapping will create irregular cells at the boundary surface and may increase the skewness of the domain and affect the results. To remedy this, layers can be added that will smooth this interface.</p>	

The .stl files that were used to construct the domain were built to a half-size scale and as a result, it was necessary to use the *transformPoints* function in *OpenFOAM* to return the domain to its real size. Porous domains were defined in the mesh generation through the use of the *topoSetsDict* dictionary, which were then converted to zones using the *setsToZones* function. The final mesh generated through the above method is displayed in Fig. 28 with the front face culled to allow viewing of the root architecture.

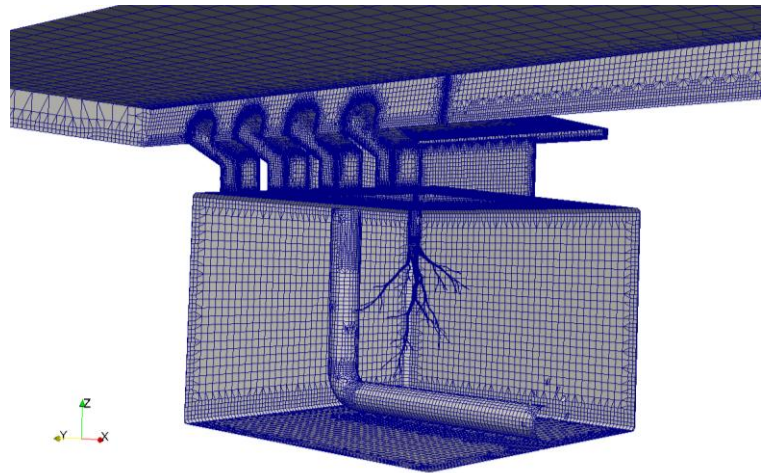


Fig. 28 – Full 3D Simulation Mesh with Inlets, Outlet Pipe and Roots

The *setFields* function was again used to define the initial *alpha1* and velocity (*U*) field as adopted in the 3D inlet modelling. Fig. 29 shows a slice of the mesh which highlights the irregular shapes generated by the *snappyHexMesh* utility and the difficulty of assigning fluid properties to such a mesh. The mesh was checked prior to running the *porousInterFoam* code and was found to pass the mesh check. After several hours running in parallel, however the simulation had failed to advance beyond a time $t=0.001s$ and the *deltaT* value, arising from adjustable run time in the *controlDict* had decreased to just $10^{-17}s$, after it was initially set at $10^{-3}s$.

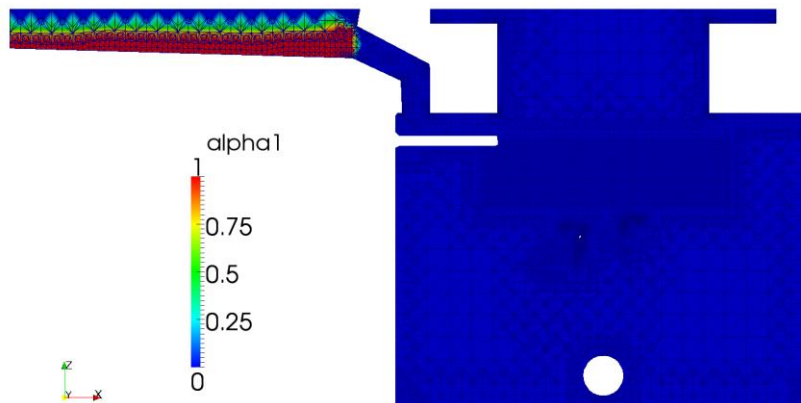


Fig. 29 – Slice from 3D Simulation Displaying *Alpha1* Field

The adjustable run time function is used in the *controlDict* dictionary in transient codes such as *porousInterFoam* in order to control the courant number, which is an indirect measure of the stability of the system. Its value is limited by entries in the *controlDict*. Further reviews were made of the *snappyHexMeshDict* in order to generate a smoother mesh, but this was unsuccessful. It is suspected that the reason for the simulation crash was due to poor mesh quality which led to a Raleigh-Taylor instability, where the interaction of two fluids of different densities is dictated by the movement of the lighter fluid. An example of this would be draining a bottle of water where air rises through the water and into the bottle at a faster rate than the water leaves the bottle.

7. Conclusions & Discussion

In summary, the present work has demonstrated an in depth understanding of the basic physical principles which govern multiphase flow. These concepts have been developed through the use of the CFD package *OpenFOAM* in the context of a *Hydro Filterra* bioretention system installed by *Hydro International* at a site in Barry, South Wales.

The initial phase of simulations demonstrated that the inlet condition of the unit can be simplified into a 2-dimensional structure. Analysis was conducted using the Eulerian VOF method of solving two phase flow as handled by *interFoam* and *porousInterFoam*. Validation of these codes has been provided in the literature [10] and through work by others within the project group [6]. It was shown that the energy dissipating stone which sits at the soil surface is central to governing flow and there is room for further investigation into its optimisation. The conclusion can be drawn that water should be allowed to drain from both sides to optimise drainage. Suggestions for experimental procedures which would validate the findings of the computational simulation have been addressed and are also discussed in section 8.

The combination of free surface flow and porous media has been investigated and it has been found that a reasonable 3-dimensional analogue can be achieved using *blockMesh* to replicate drainage into a single inlet gully. Further work is however required to develop a case whereby fluid flow across the face of the inlet is accounted for, procedures and suggestions for this development are proposed in section 8. Additional development is required to generate a more appropriate mesh for the full-scale 3D model of the installation unit. Pavey [6] has conducted mesh studies that show the software *PointWise* may be a more suitable candidate.

8. Project Evaluation & Further Work

Generally, this project has shown great success, with significant achievements in the 2D and 3D modelling. The majority of the initial objectives have been met, with the exception of the full scale 3D model. Simulations were also restricted to a single inlet flow condition namely maximum treatable inlet flow. Mesh generation has been at the centre of this project and work has been conducted at the limit of the capabilities of *blockMesh*, the *OpenFOAM* mesh generator.

A number of potential fields are available for further study within this project. For example, the *porousInterFoam* code does not account for changes in porosity due to media saturation. There is potential to develop a function similar to *groovyBC* that will change the resistance to the flow over time dependent on the saturation of the porous media.

A new method of mesh generation could be adopted in order to resolve the Raleigh-Taylor instability as discussed in section 6. Preliminary work suggests that *PointWise* may generate the best mesh for this case due to its use of regular tetrahedral cells, which are superior to the snapping of cells to surfaces used by *snappyHexMesh*.

An additional field of development is to generate a case whereby the fluid behaviour at the street level, adjacent to the unit is handled in a physically more accurate manner. To this end, a method of developing a cross-flow condition across the face of the drain inlet should be developed. This may be achieved through augmentation of the *setFields* dictionary or *groovyBC* to maintain a constant U_z velocity which is not immediately overcome by the effect of water draining towards the curb as has been observed in the present work.

Furthermore, the fluid behaviour in the porous region could be experimentally tested using DIC as discussed in section 4.4. This would provide empirical data to validate the findings of this report. Additional experimentation could be conducted to determine the influence of the energy dissipating stone replicating the unit in laboratory conditions and changing its dimensions to optimise drainage efficiency.

References

- [1] – Tabor, G., Begley, A., Pavey, S., Please, J., Ronald, J., Russell, S., Tarrant, J., Whitehurst, L., Winston-Gore, S. (2011) *Investigating Stormwater Filters and Bioretention Systems*, Group Project Report G1, College of Engineering, Mathematics and Physical Sciences, University of Exeter.
- [2] – Tarrant, J. (2011) *Macro Scale Computational Analysis of the Hydro Filterra Storm Water Drainage System in an Industrial Urban Environment*, Individual Project Report I1, College of Engineering, Mathematics and Physical Sciences, University of Exeter.
- [3] – Tabor, G., Begley, A., Pavey, S., Please, J., Ronald, J., Russell, S., Tarrant, J., Whitehurst, L., Winston-Gore, S. (2012) *Investigating Stormwater Filters and Bioretention Systems*, Group Project Report G2, College of Engineering, Mathematics and Physical Sciences, University of Exeter.
- [4] – http://www.hydro-international.biz/index_uk.php - accessed 4th November 2011.
- [5] – http://cms.esi.info/Media/productImages/28683_1313421457846_PF.jpg - accessed 8th November 2011.
- [6] – Pavey, S. (2012) *Macro Scale Computational Analysis Including Porous Media and Free Surface Interaction*, Individual Project Report I2, College of Engineering, Mathematics and Physical Sciences, University of Exeter.
- [7] – Ronald, J. (2012) *Computational Modelling of Plant Root Architecture and Fluid Absorption through Filtration Media Populated by Root Structures*, Individual Report I2, College of Engineering, Mathematics and Physical Sciences, University of Exeter.
- [8] – Lipeme Kouyi, G., Fraisse, D., Rivière, N., Guinot, V., Chocat, B. (2008) *1D Modelling of the Interactions between Heavy Rainfall-Runoff in Urban Area and Flooding Flows from Sewer Network and River*, 11th International Conference on Urban Drainage, Edinburgh, Scotland, UK, 2008.
- [9] – Leandro, J., A. Chen, S. Djordjević and D.A. Savic (2009) *A Comparison of 1D/1D and 1D/2D Coupled (Sewer/Surface) Hydraulic Models for Urban Flood Simulation*, Journal of Hydraulic Engineering, ASCE Volume 135, Issue 6, pp. 495-504.
- [10] – Djordjević, S., Saul, A., Tabor, G., Blanksby, J., Galambos, I., Sabtu, I., Sailor, G. (2011) *Experimental and Numerical Investigation of Interactions between above and below ground Drainage Systems*, 12th International Conference on Urban Drainage, Porto Alegre/Brazil, 10-15 September 2011.
- [11] – Jarman, D., Faram, M., Butler, D., Tabor, G., Stovin, V., Burt, D., Throp, E. (2008) *Computational Fluid Dynamics as a tool for Urban Drainage System Analysis: A Review of Applications and Best Practice*, 11th International Conference on Urban Drainage, Edinburgh, Scotland, UK, 2008.
- [12] – Oberkampf and Trucano (2002) *Verification and Validation in Computational Fluid Dynamics*.
- [13] – Faram and Harwood (2000) *CFD for the Water Industry; The Role of CFD as a Tool for the Development of Wastewater Treatment Systems*, Fluent Users' Seminar 2000, Sheffield, UK, 21-22 September, Paper 1-1.
- [14] – Mignot, E. (2005) *Etude expérimentale et numérique de l'inondation d'une zone urbanisée : cas des écoulements dans les carrefours en croix*, PhD Thesis, Ecole Centrale de Lyon, France, pp. 333.

- [15] – Faram and Harwood (2002), *Assessment of the Effectiveness of Stormwater Treatment Chambers using Computational Fluid Dynamics*, 9th International Conference on Urban Drainage, Portland, Oregon, USA, 9-13 September 2002.
- [16] – Bardiaux, J., Mosé, R., Vazquez, J., Wertel, J. (2008), *Two Turbulent Flow 3D-Modellings to Improve Sewer Net Instrumentation*, 11th International Conference on Urban Drainage, Edinburgh, Scotland, UK, 2008.
- [17] – Tabor, G. (2010) *OpenFOAM: An Exeter Perspective*, V European Conference on Computational Fluid Dynamics, ECCOMAS CFD, 2010.
- [18] – Winston-Gore, S. (2012) *Investigating the Wide Scale Impact of Integrating a Hydro Filterra Bioretention System within an Urban Drainage Network Using Computational Models*, Individual Project Report I2, College of Engineering, Mathematics and Physical Sciences, University of Exeter.
- [19] – Brackbill, J., Kothe, D. B., Zemach, C. (1992) *A Continuum Method for Modelling Surface Tension*, Journal of Computational Physics, 100: 335-354.
- [20] – *Hydro Filterra Performance Data*, *Hydro International*
- [21] – *Hydro Filterra Drawings*, supplied by *Hydro International*
- [22] – www.engineeringtoolbox.com/hydraulic-equivalent-diameter-d_458.html - accessed 4th February 2012.
- [23] – Tabor, G. (2011) *ECMM106 – Computational Modelling: Tutorial 1* College of Engineering, Mathematics and Physical Sciences, University of Exeter.
- [24] – www.cfd-online.com/Wiki/Turbulence_intensity - Accessed 4th February 2012.
- [25] – Tabor, G. (2011) *ECMM106 – Computational Modelling: Tutorial 2* College of Engineering, Mathematics and Physical Sciences, University of Exeter.
- [26] – Begley, A. (2012) *Three Dimensional Image Based Meshing and Computational Analysis of Fluid Flow in Various Porous Media*, Individual Project Report I2, College of Engineering, Mathematics and Physical Sciences, University of Exeter.
- [27] – Please, J. (2012) *Micro Scale Experimental Investigation to Determine the Hydraulic Properties of the Hydro Filterra Bioretention System with Comparison to Tests on a Rapid-Prototype Sample and Computer Model Based on Micro-CT Scans*, Individual Project Report I2, College of Engineering, Mathematics and Physical Sciences, University of Exeter.
- [28] – Lee, S-J. & Kim, H-B. (1999) *Laboratory Measurements of Velocity and Turbulence Field Behind Porous Fences*. Department of Mechanical Engineering, Advanced Fluids Engineering Research Center, Pohang University of Science and Technology, Pohang 790-784, South Korea.
- [29] – Delnoij, E., Kuipers, J. A. M. and van Swaaij, W. P. M. (1997) *Computational Fluid Dynamics Applied to Gas-Liquid Contactors*, Chemical Engineering Science, Vol. 52, No. 21, pp. 3623-3638.